PHYSICAL REVIEW D **88,** 105017 (2013)

Charmonia and bottomonia in a magnetic field

Jeremy Alford and Michael Strickland
Department of Physics, Kent State University, Kent, Ohio 44242, USA
(Received 15 September 2013; published 14 November 2013)

We study the effect of a static homogeneous external magnetic field on charmonium and bottomonium states. In an external magnetic field, quarkonium states do not have a conserved center-of-mass momentum. Instead there is a new conserved quantity called the pseudomomentum which takes into account the Lorentz force on the particles in the system. When written in terms of the pseudomomentum, the internal and center-of-mass motions do not decouple and, as a result, the properties of quarkonia depend on the states' center-of-mass momentum. We analyze the behavior of heavy particle-antiparticle pairs subject to an external magnetic field assuming a three-dimensional harmonic potential and Cornell potential plus spin-spin interaction. In the case of the Cornell potential, we also take into account the mixing of the η_c and J/ψ states and η_b and Υ states due to the background magnetic field. We then numerically calculate the dependence of the masses and mixing fractions on the magnitude of the background magnetic field and center-of-mass momentum of the state.

DOI: 10.1103/PhysRevD.88.105017 PACS numbers: 11.15.Bt, 04.25.Nx, 11.10.Wx, 12.38.Mh

I. INTRODUCTION

The behavior of matter subject to magnetic fields has been a subject of interest for physicists for quite some time. Already over one hundred years ago Zeeman showed that an external magnetic field affected the spectrum of light emitted by a flame [1–3]. In recent years there has been considerable attention focused on the question of what happens to matter in the presence of extremely strong magnetic fields which are many orders of magnitude larger than normally experienced magnetic fields. There are at least two situations in which extremely strong magnetic fields are expected to be generated: (1) During early times after noncentral heavy ion collisions one expects $B \sim m_\pi^2 \sim 10^{18}$ G at energies probed by the Relativistic Heavy Ion Collider and $B \sim 15 m_\pi^2 \sim 1.5 \times 10^{19}$ G at Large Hadron Collider (LHC) energies [4–9] and (2) in the interior of magnetars, which are a class of neutron stars which possess central magnetic fields on the order of 10^{18}–10^{19} G [10]. In this paper, we study the behavior of charmonium and bottomonium states subject to magnetic fields with an eye towards applications to the phenomenology of relativistic heavy ion collisions.

Interest in the effects of strong magnetic fields in heavy ion collisions has become a hot topic recently following the prediction of a nontrivial quantum chromodynamics (QCD) effect dubbed "the chiral magnetic effect" which stems from small P- and CP-odd interactions inducing an electromagnetic current when a quark-gluon plasma is placed in an external magnetic field [4]. There has been much work related to this in recent years and in addition it has been shown how to self-consistently take into account this effect through Berry curvature flux in the presence of a magnetic field [11,12]. The existence of such high magnetic fields has also prompted many research groups to study how the finite temperature deconfinement and chiral phase transitions are affected by the presence of a strong background magnetic field. These studies have included direct numerical investigations using lattice QCD [13–17] and theoretical investigations using a variety of methods including, for example, perturbative QCD studies, model studies, and string-theory-inspired anti–de Sitter/conformal field theory correspondence studies [18–43].

In this paper, we consider the effects of magnetic fields on heavy quarkonium states, focusing on $1s$ charmonium and bottomonium states. The physics of quantum mechanical bound states in a background magnetic field is complicated by the fact that in a background magnetic field the center-of-mass (COM) momentum is not a conserved quantity due to the breaking of translational invariance by the vector potential. Instead one must take into account the Lorentz force on the constituents and construct a quantity called the COM pseudomomentum [44–57]. However, in practice one finds that, even after expressing the Hamiltonian in terms of the pseudomomentum, it is not possible to factorize the Hamiltonian into free COM motion plus decoupled internal motion. As a result, the spectrum of a bound state in a background magnetic field depends on the COM momentum of the system. To the best of our knowledge, the first theoretical consideration of motional effects was by Lamb [46] and, as we will show, this effect is related to the so-called motional Stark effect.

In this paper we investigate the effect of strong magnetic fields on heavy quarkonium states including such motional effects. Heavy quarkonium is a nice test bed for QCD since heavy quark states are dominated by short-distance physics and can be treated using heavy quark effective theory [58]. Based on such effective theories of QCD, nonrelativistic quarkonium states can be reliably described. Their binding energies are much smaller than the quark mass $m_q \gg \Lambda_{\rm QCD}$ ($q = c,\ b$), and their sizes are much larger than $1/m_q$. Since the velocity of the quarks in the bound state

is small ($v \ll c$), quarkonium can be understood in terms of nonrelativistic potential models such as the Cornell potential which can be derived directly from QCD using effective field theory [59–61].

We present numerical calculations using a Cornell potential supplemented by a spin-spin interaction which allows for a splitting between the spin-singlet and spin-triplet states. This study contributes to ongoing discussions of the effect of strong magnetic fields on QCD bound states [62–68]. Apart from the long-range interactions, which are fundamentally different, the physics of heavy quarkonium is very similar to positronium [69–81].[1] In addition to motional effects [81], it is also necessary to take into account the hyperfine mixing in the background magnetic field. In positronium this results in a change of the spin-singlet and spin-triplet energy eigenvalues and "quenching" of orthopositronium 3γ decays [76,77,79]. Analogous effects occur in quarkonium and we present quantitative calculations of the effect utilizing a realistic heavy quark interaction potential. In addition, we present exact analytic formulas which can be obtained assuming a harmonic interaction between the constituents. The harmonic interaction results are used for purposes of discussion and also to check the numerical methods which are applied in the more realistic case.

The structure of the paper is as follows. In Sec. II we introduce the pseudomomentum. In Sec. III we discuss the application to two particle states and then specialize to the case of particle-antiparticle states. In Sec. IV we discuss the relation of the pseudopotential derived in the previous section to the motional Stark effect. In Sec. V we discuss the prescription we use to subtract the energy associated with the center-of-mass motion. In Sec. VI we discuss the mixing of the spin-singlet and spin-triplet states in the presence of a magnetic field. In Sec. VII we present the potential we use for our final results. In Sec. VIII we present our numerical results. In Sec. IX we present our conclusions and outlook for the future. In three appendixes we collect details of the interquark potential used and resulting spectra, our numerical method for solving the 3D Schrödinger equation, and an investigation of what happens to a harmonic state with a given center-of-mass momenta when a magnetic field is turned on suddenly.

II. PARTICLE IN A CONSTANT MAGNETIC FIELD

We begin with the basics by introducing the pseudomomentum in the context of a single classical nonrelativistic charged spin one-half particle in a background magnetic field. As we will demonstrate, unlike the particle momentum, the pseudomomentum is conserved since it takes into account the Lorentz force on the particle. The classical nonrelativistic Hamiltonian for a particle in a constant magnetic field can be written

$$\mathcal{H} = \frac{1}{2m}[\mathbf{p} - q\mathbf{A}(\mathbf{r})]^2 + V(\mathbf{r}) - \boldsymbol{\mu}\cdot\mathbf{B} + m, \quad (1)$$

where m is the rest mass of the particle and we assume $\mathbf{B}(\mathbf{x}) = (0, 0, B)$ which, in symmetric gauge, can be expressed in terms of the vector potential $\mathbf{A}(\mathbf{r}) = \frac{1}{2}\mathbf{B}\times\mathbf{r} = \frac{1}{2}B(-y, x, 0)$.

We can apply Hamilton's equations to derive the equation of motion

$$-\frac{\partial\mathcal{H}}{\partial r_i} = \dot{p}_i, \qquad \frac{\partial\mathcal{H}}{\partial p_i} = \dot{r}_i. \quad (2)$$

The second Hamilton equation gives $m\dot{r}_i = p_i - qA_i$ which allows us to solve for the canonical momentum, $p_i = m\dot{r}_i + qA_i$. Using this, we can evaluate the full time derivative of the canonical momentum

$$\begin{aligned}\dot{p}_i &= m\ddot{r}_i + q\left(\frac{\partial A_i}{\partial t} + \frac{dr_j}{dt}\frac{\partial A_i}{\partial r_j}\right),\\ &= m\ddot{r}_i + q\dot{r}_j\frac{\partial A_i}{\partial r_j},\end{aligned} \quad (3)$$

where, in going from the first to second line we have used the fact that the vector potential is static in the case under consideration. The right-hand side of the first Hamilton equation gives

$$\begin{aligned}-\frac{\partial\mathcal{H}}{\partial r_i} &= \frac{1}{m}(\mathbf{p} - q\mathbf{A}(\mathbf{r}))\cdot\left(q\frac{\partial\mathbf{A}}{\partial r_i}\right) - \frac{\partial V}{\partial r_i},\\ &= q\dot{r}_j\frac{\partial A_j}{\partial r_i} - \frac{\partial V}{\partial r_i}.\end{aligned} \quad (4)$$

Equating the two sides we obtain

$$m\ddot{r}_i = q\dot{r}_j\frac{\partial A_j}{\partial r_i} - q\dot{r}_j\frac{\partial A_i}{\partial r_j} - \frac{\partial V}{\partial r_i}. \quad (5)$$

Using $\mathbf{v}\times\mathbf{B} = \dot{\mathbf{r}}\times(\nabla\times\mathbf{A}) = \nabla(\dot{\mathbf{r}}\cdot\mathbf{A}) - (\dot{\mathbf{r}}\cdot\nabla)\mathbf{A}$ we can rewrite this as

$$m\ddot{\mathbf{r}} = q\dot{\mathbf{r}}\times\mathbf{B} - \nabla V. \quad (6)$$

In the case that there is no potential, $V = 0$, we have only the Lorentz force acting on the particle

$$m\ddot{\mathbf{r}} = q\dot{\mathbf{r}}\times\mathbf{B}, \quad (7)$$

which shows that the momentum is not conserved in a constant magnetic field, as expected; however, we can introduce a quantity which is conserved called the *pseudomomentum*, $\mathcal{K}$,

$$\begin{aligned}\mathcal{K} &= m\dot{\mathbf{r}} + q\mathbf{B}\times\mathbf{r},\\ &= \mathbf{p} + \frac{q}{2}\mathbf{B}\times\mathbf{r},\\ &= \mathbf{p} + q\mathbf{A},\end{aligned} \quad (8)$$

such that the equation of motion can be expressed as

$$\frac{d}{dt}\mathcal{K} = 0. \quad (9)$$

[1] For a nice review of positronium physics see Ref. [82].

III. TWO COUPLED PARTICLES IN A CONSTANT MAGNETIC FIELD

We next consider the case of two particles subject to a translationally invariant potential in nonrelativistic quantum mechanics. We will follow closely the treatment found in Ref. [55]. The Hamiltonian operator for two particles in a constant magnetic field can be written as

$$\mathcal{H} = \frac{1}{2m_1}[\mathbf{p}_1 - q_1\mathbf{A}(\mathbf{r}_1)]^2 + \frac{1}{2m_2}[\mathbf{p}_2 - q_2\mathbf{A}(\mathbf{r}_2)]^2 + V(\mathbf{r}_1 - \mathbf{r}_2) - \boldsymbol{\mu}\cdot\mathbf{B} + m_1 + m_2, \tag{10}$$

where $\boldsymbol{\mu} = \boldsymbol{\mu}_1 + \boldsymbol{\mu}_2$ is the sum of the two particles' magnetic moments and $\mathbf{B}(\mathbf{x}) = (0, 0, B)$, which can be expressed in terms of the vector potential $\mathbf{A}(\mathbf{r}) = \frac{1}{2}\mathbf{B}\times\mathbf{r} = \frac{1}{2}B(-y, x, 0)$ in symmetric gauge. As usual, $\mathbf{p}_i = -i\nabla$ is the momentum operator for the ith particle. As in the previous section, one finds that the COM momentum of the system is no longer conserved. This is due to the breaking of translational invariance by the vector potential (changing the origin changes $\mathbf{A}$). In order to preserve translational invariance in a constant magnetic field an additional gauge transformation is required. This can be achieved by introducing the generalized pseudomomentum operator [55]

$$\mathcal{K}_k = \sum_{j=1}^{2}\left(-i\frac{\partial}{\partial x_{jk}} - q_j\int_0^{\mathbf{r}_j}\frac{\partial\mathbf{A}}{\partial x_k}\cdot d\mathbf{r}\right), \tag{11}$$

where $k = 1, 2, 3$ denotes Cartesian components. Integrating and discarding a constant one obtains

$$\mathcal{K} = \sum_{j=1}^{2}(\mathbf{p}_j - q_j\mathbf{A}_j + q_j\mathbf{B}\times\mathbf{r}_j). \tag{12}$$

In the gauge used herein we have $\mathbf{A}(\mathbf{r}) = \frac{1}{2}\mathbf{B}\times\mathbf{r}$ which allows us to simplify this to

$$\begin{aligned}\mathcal{K} &= \sum_{j=1}^{2}\left(\mathbf{p}_j + \frac{1}{2}q_j\mathbf{B}\times\mathbf{r}_j\right),\\ &= \sum_{j=1}^{2}(\mathbf{p}_j + q_j\mathbf{A}_j),\end{aligned} \tag{13}$$

which is the generalization of the one particle case obtained in the previous section. One can verify explicitly that the pseudomomentum operator commutes with the Hamiltonian

$$[\mathcal{K}, \mathcal{H}] = 0. \tag{14}$$

One can also compute the commutator of two components of $\mathcal{K}$ in which case one obtains

$$[\mathcal{K}_k, \mathcal{K}_l] = -i\varepsilon_{klm}B_m\left(\sum_{j=1}^{2}q_j\right), \tag{15}$$

which means that one will only be able to determine all components of $\mathcal{K}$ simultaneously for an electric charge neutral system.

A. Two particles with equal and opposite charge

In this section we specialize to the case that $q_1 = -q_2 = q$. To proceed we introduce center-of-mass and relative coordinates

$$\mathbf{R} = \frac{m_1\mathbf{r}_1 + m_2\mathbf{r}_2}{M}, \qquad \mathbf{r} = \mathbf{r}_1 - \mathbf{r}_2, \tag{16}$$

where $M = m_1 + m_2$. As is standard, we can express the individual positions as

$$\mathbf{r}_1 = \mathbf{R} + \frac{m_r}{m_1}\mathbf{r}, \qquad \mathbf{r}_2 = \mathbf{R} - \frac{m_r}{m_2}\mathbf{r}, \tag{17}$$

where $m_r = m_1m_2/M$ is the reduced mass.

This allows us to simplify the pseudomomentum operator

$$\begin{aligned}\mathcal{K} &= \sum_{j=1}^{2}\left(\mathbf{p}_j + \frac{1}{2}q_j\mathbf{B}\times\mathbf{r}_j\right),\\ &= -i\left(\frac{\partial}{\partial\mathbf{r}_1} + \frac{\partial}{\partial\mathbf{r}_2}\right) + \frac{1}{2}q\mathbf{B}\times(\mathbf{r}_1 - \mathbf{r}_2),\\ &= -i\frac{\partial}{\partial\mathbf{R}} + \frac{1}{2}q\mathbf{B}\times\mathbf{r}.\end{aligned} \tag{18}$$

Since the system is neutral, the full two-particle eigenfunctions Φ of the Hamiltonian are simultaneous eigenfunctions of all components $\mathcal{K}_i$ of the pseudomomentum with eigenvalues K_i. This allows us to factorize the full wave function

$$\begin{aligned}\Phi(\mathbf{R}, \mathbf{r}) &= \exp\left[i\left(\mathbf{K} - \frac{1}{2}q\mathbf{B}\times\mathbf{r}\right)\cdot\mathbf{R}\right]\Psi(\mathbf{r})\\ &\equiv \phi(\mathbf{R}, \mathbf{r})\Psi(\mathbf{r}),\end{aligned} \tag{19}$$

which satisfies $\mathcal{K}_j\Phi = K_j\Phi$ by construction.

Expanding out the two-particle Hamiltonian one finds the "relative" Hamiltonian

$$\mathcal{H}_{\text{rel}} = \frac{\mathbf{K}^2}{2M} - \frac{q}{M}(\mathbf{K}\times\mathbf{B})\cdot\mathbf{r} + \frac{\mathbf{p}^2}{2m_r} + \frac{q}{2}\left(\frac{1}{m_1} - \frac{1}{m_2}\right)\mathbf{B}\cdot(\mathbf{r}\times\mathbf{p}) + \frac{q^2}{8m_r}(\mathbf{B}\times\mathbf{r})^2 + V(\mathbf{r}) - \boldsymbol{\mu}\cdot\mathbf{B} + m_1 + m_2, \tag{20}$$

where $\mathbf{p} = -i\nabla$ is the relative momentum operator and one has the new eigenvalue equation $\mathcal{H}_{\text{rel}}\Psi(\mathbf{r}) = E\Psi(\mathbf{r})$. Note that, unlike the case without the external field, the energy eigenvalue E depends on the value of $\mathbf{K}$ through coupling in the second term and not only through the term $\mathbf{K}^2/2M$.

B. Heavy-light system

In the limit that $m_2 \to \infty$ while holding m_1 fixed, we have $M \to \infty$ and $m_r = m_1 \equiv m$ and we obtain

$$\mathcal{H}_{\text{rel}} = \frac{\mathbf{p}^2}{2m} - \frac{q}{2m}\mathbf{B}\cdot(\mathbf{r}\times\mathbf{p}) + \frac{q^2}{8m}(\mathbf{B}\times\mathbf{r})^2 + V(\mathbf{r}) - \boldsymbol{\mu}\cdot\mathbf{B} + m, \tag{21}$$

where we have discarded the infinite constant m_2 in this case. Recalling that $\mathbf{A} = \frac{1}{2}\mathbf{B}\times\mathbf{r} = \frac{1}{2}B(-y, x, 0)$ one has $(\mathbf{B}\times\mathbf{r})^2 = B^2\rho^2$ and using $\mathbf{B}\cdot(\mathbf{r}\times\mathbf{p}) = (\mathbf{B}\times\mathbf{r})\cdot\mathbf{p} = \rho B p_\phi = -iB\partial_\phi$ we obtain

$$\mathcal{H}_{\rm rel} = -\frac{1}{2m}\nabla^2 + \frac{i}{2}\omega_c\frac{\partial}{\partial\phi} + \frac{m\omega_c^2}{8}\rho^2 + V(\mathbf{r}) - \boldsymbol{\mu}\cdot\mathbf{B} + m, \tag{22}$$

where $\omega_c = qB/m$. This is the standard nonrelativistic Hamiltonian for a spin-one-half particle subject to a potential V and an external magnetic field.

C. Particle-antiparticle pair

For a bound state consisting of a particle-antiparticle pair we have $m_1 = m_2 = m$, $M = 2m$, and $m_r = m/2$. In this case the relative Hamiltonian simplifies to

$$\mathcal{H}_{\rm rel} = \frac{\mathbf{K}^2}{2M} - \frac{q}{M}(\mathbf{K}\times\mathbf{B})\cdot\mathbf{r} - \frac{\nabla^2}{2m_r} + \frac{q^2}{8m_r}(\mathbf{B}\times\mathbf{r})^2 + V(\mathbf{r}) - \boldsymbol{\mu}\cdot\mathbf{B} + M. \tag{23}$$

Next we decompose $\mathbf{K} = K_x\hat{\mathbf{x}} + K_y\hat{\mathbf{y}} + K_z\hat{\mathbf{z}}$ and simplify the expression above to obtain

$$\mathcal{H}_{\rm rel} = \frac{\mathbf{K}^2}{2M} + \frac{qB}{4m_r}K_x y - \frac{qB}{4m_r}K_y x - \frac{\nabla^2}{2m_r} + \frac{q^2B^2}{8m_r}\rho^2 + V(\mathbf{r}) - \boldsymbol{\mu}\cdot\mathbf{B} + M. \tag{24}$$

1. Relation between the pseudomomentum and kinetic center-of-mass momentum

We now derive a general relation between the pseudomomentum and kinetic COM momentum. The COM kinetic momentum of the system is given by

$$\mathbf{P}_{\rm kinetic} = \sum_j\left(-i\frac{\partial}{\partial\mathbf{r}_j} - q_j\mathbf{A}_j\right), = -i\frac{\partial}{\partial\mathbf{R}} - \frac{1}{2}q\mathbf{B}\times\mathbf{r}. \tag{25}$$

Therefore, we have

$$\langle\mathbf{P}_{\rm kinetic}\rangle = \frac{\int_{\mathbf{R}}\int_{\mathbf{r}}\Phi^*[-i\frac{\partial}{\partial\mathbf{R}} - \frac{1}{2}q\mathbf{B}\times\mathbf{r}]\Phi}{\int_{\mathbf{R}}\int_{\mathbf{r}}\Phi^*\Phi}. \tag{26}$$

Using

$$-i\frac{\partial}{\partial\mathbf{R}}\Phi = \left(\mathbf{K} - \frac{1}{2}q\mathbf{B}\times\mathbf{r}\right)\Phi, \tag{27}$$

one finds

$$\langle\mathbf{P}_{\rm kinetic}\rangle = \mathbf{K} - q\mathbf{B}\times\langle\mathbf{r}\rangle. \tag{28}$$

D. Particle-antiparticle pair with a harmonic interaction

We now specialize to the case that the potential is harmonic in which case the wave functions and energy levels can be obtained analytically. Some of the results contained in this subsection were first obtained explicitly by Herold *et al.* [55]. We repeat the derivation here in order to use them as a basis for discussion of the COM momentum dependence of the energy. We also use this case as a check for our numerics since it can be solved analytically.

Using the general relative Hamiltonian for a particle-antiparticle pair (24) and $V(\mathbf{x}) = \frac{1}{2}k\mathbf{x}^2 = \frac{1}{2}m_r\omega_0^2(x^2 + y^2 + z^2)$ we have

$$\begin{aligned}\mathcal{H}_{\rm rel} &= \frac{\mathbf{K}^2}{2M} - \frac{\nabla^2}{2m_r} + \frac{1}{2}m_r\left(\omega_0^2 + \frac{\omega_c^2}{4}\right)(x^2+y^2) - \frac{\omega_c K_y}{4}x + \frac{\omega_c K_x}{4}y + \frac{1}{2}m_r\omega_0^2 z^2 - \boldsymbol{\mu}\cdot\mathbf{B} + M,\\ &= \frac{\mathbf{K}^2}{2M} - \frac{\nabla^2}{2m_r} + \frac{1}{2}a(x^2+y^2) - bx + cy + \frac{1}{2}dz^2 - \boldsymbol{\mu}\cdot\mathbf{B} + M,\end{aligned} \tag{29}$$

where $\omega_c = qB/m_r$, $\boldsymbol{\mu} = \boldsymbol{\mu}_1 + \boldsymbol{\mu}_2$, $a = m_r(\omega_0^2 + \omega_c^2/4)$, $b = \omega_c K_y/4$, $c = \omega_c K_x/4$, and $d = m_r\omega_0^2$. We can rewrite the third, fourth, and fifth terms using

$$\frac{1}{2}a(x^2+y^2) - bx + cy = \frac{1}{2}a\left[\left(x - \frac{b}{a}\right)^2 + \left(y + \frac{c}{a}\right)^2\right] - \frac{1}{2a}(b^2 + c^2). \tag{30}$$

We can simplify things further by making use of a constant coordinate shift $\bar{x} \equiv x - b/a$ and $\bar{y} \equiv y + c/a$,

$$\mathcal{H}_{\rm rel} = \frac{\mathbf{K}^2}{2M} - \frac{\nabla^2}{2m_r} + \frac{1}{2}a(\bar{x}^2 + \bar{y}^2) + \frac{1}{2}dz^2 - \frac{1}{2a}(b^2 + c^2) - \boldsymbol{\mu}\cdot\mathbf{B} + M, \tag{31}$$

which suggests that we use cylindrical coordinates with $\bar{x} = \rho\cos\phi$, $\bar{y} = \rho\sin\phi$, and $z = z$. After this, the eigenvalue equation $\mathcal{H}_{\rm rel}\Psi = E\Psi$ becomes

$$\left(-\frac{\nabla^2}{2m_r} + \frac{1}{2}a\rho^2 + \frac{1}{2}cz^2\right)\Psi(\mathbf{r}) = \left(E - \frac{\mathbf{K}^2}{2M} + \frac{b^2}{2a} + \boldsymbol{\mu}\cdot\mathbf{B} + M\right)\Psi(\mathbf{r}). \tag{32}$$

Factorizing the relative wave function as $\Psi(\mathbf{r}) = e^{i\ell\phi}Z(z)\psi(\rho)$ we find

$$\left(-\frac{\partial^2}{\partial\rho^2} - \frac{1}{\rho}\frac{\partial}{\partial\rho} + \frac{|\ell|^2}{\rho^2} + \alpha^4\rho^2\right)\psi = 2m_r\lambda\psi, \tag{33}$$

where $\alpha^2 = \sqrt{m_r a} = m_r\sqrt{\omega_0^2 + \omega_c^2/4}$, $\lambda = E - E_z - \mathbf{K}^2/2M + (b^2 + c^2)/2a + \boldsymbol{\mu}\cdot\mathbf{B} + M$, and E_z is the eigenvalue of the separated z equation

$$\left(-\frac{\partial^2}{\partial z^2} + \gamma^4 z^2\right)Z = 2m_r E_z Z, \tag{34}$$

where $\gamma = (m_r c)^{1/4} = \sqrt{m_r\omega_0}$ which has a solution

$$Z = Ne^{-\frac{1}{2}\gamma^2 z^2} H_{n_z}(\gamma z), \tag{35}$$

and energy eigenvalue

$$E_z = \left(n_z + \frac{1}{2}\right)\omega_0. \tag{36}$$

Convergence as $\rho \longrightarrow \infty$ requires

$$\lambda = \frac{\alpha^2}{m_r}(2n_\perp + 1 + |\ell|) = (2n_\perp + 1 + |\ell|)\sqrt{\omega_0^2 + \frac{\omega_c^2}{4}}. \tag{37}$$

Solving for E we obtain the energy eigenvalues for the system

$$E_{\mathbf{K},n_\perp n_z \ell} = \frac{\mathbf{K}^2}{2M} - \frac{\omega_c^2(K_x^2 + K_y^2)}{32m_r(\omega_0^2 + \omega_c^2/4)} + \left(n_z + \frac{1}{2}\right)\omega_0 + (2n_\perp + 1 + |\ell|)\sqrt{\omega_0^2 + \frac{\omega_c^2}{4}} - \boldsymbol{m_r}\cdot\mathbf{B} + M. \tag{38}$$

We can now write the full two-particle wave function

$$\Phi_{\mathbf{K},n_\perp n_z \ell}(\mathbf{R},\mathbf{r}) = \mathcal{N}\rho^{|\ell|}e^{i\ell\phi}e^{-\frac{1}{2}\gamma^2 z^2}e^{-\frac{1}{2}\alpha^2\rho^2}H_{n_z}(\gamma z) \times L_{n_\perp}^{|\ell|}(\alpha^2\rho^2)e^{i(\mathbf{K}-\frac{1}{2}q\mathbf{B}\times\mathbf{r})\cdot\mathbf{R}}, \tag{39}$$

where $\mathcal{N}$ is a normalization constant and

$$\omega_c = \frac{qB}{m_r}, \quad \alpha^2 = m_r\sqrt{\omega_0^2 + \frac{\omega_c^2}{4}}, \quad \beta = \frac{\omega_c}{4m_r(\omega_0^2 + \omega_c^2/4)}, \quad \gamma^2 = m_r\omega_0, \quad \rho^2 = (x - \beta K_y)^2 + (y + \beta K_x)^2, \quad \phi = \arctan\left(\frac{y + \beta K_x}{x - \beta K_y}\right). \tag{40}$$

1. Center-of-mass kinetic momentum

Using this we can analytically compute the relationship between the pseudomomentum and the COM kinetic momentum of the state. Using Eq. (28) and

$$\mathbf{B}\times\mathbf{r} = B(-y, x, 0) = B\left(-\rho\sin\phi + \frac{c}{a}, \rho\cos\phi + \frac{b}{a}, 0\right), \tag{41}$$

one finds in this case

$$\langle\mathbf{P}_{\text{kinetic}}\rangle = \mathbf{K} - \frac{qBc}{a}\hat{\mathbf{x}} - \frac{qBb}{a}\hat{\mathbf{y}}. \tag{42}$$

Plugging in the definitions of a, b, and c we obtain

$$\langle\mathbf{P}_{\text{kinetic}}\rangle = \left(\frac{4\omega_0^2}{4\omega_0^2 + \omega_c^2}K_x, \frac{4\omega_0^2}{4\omega_0^2 + \omega_c^2}K_y, K_z\right). \tag{43}$$

As we can explicitly see from this expression, the components of the kinetic COM momentum do not directly correspond to the pseudomomentum components. We note that in Appendix C we derive this formula in a different manner by assuming a time-dependent magnetic field which turns on rapidly.

IV. RELATION TO THE MOTIONAL STARK EFFECT

One way to intuitively understand the result obtained in Eq. (24) is try to derive it in a different manner. We can instead try to write down the nonrelativistic Hamiltonian in the COM rest frame. This step is self-contradictory since, as we have pointed out previously, the COM momentum is not a conserved quantity in the presence of an external magnetic field; however, let us ignore this for the time being and assume that we can, in fact, boost to the rest frame of the state. As before, we assume that the magnetic field points in the z direction and as a result the dynamics in the z direction is straightforward. Putting the system at rest in the z direction and assuming that we can also hold it at rest in the y direction we need only consider boosts in the x direction with $v_x = P_x/M$. In the lab frame there is only a magnetic field. In the comoving frame there will be both electric and magnetic fields. Using the standard transformation laws for electric and magnetic fields one finds

$$E_x' = 0, \quad B_x' = 0, \quad E_y' = -\gamma v_x B \approx -v_x B, \quad B_y' = 0, \quad E_z' = 0, \quad B_z' = \gamma B \approx B,$$

where for the terms with $\approx$ appearing we have discarded terms of the order v_x^2 and higher.

As we can see from the relations above, if we boost to the rest frame of the state, there is an additional electric interaction of the form $H'_{\text{electric}} = -q\mathbf{E}'\cdot\mathbf{r}$ where $\mathbf{r} = \mathbf{r}_1 - \mathbf{r}_2$ is the relative position. Using the expressions above one finds trivially

$$H'_{\text{electric}} = \frac{qB}{4m_r}P_x y, \tag{44}$$

where we have used the fact that for a particle-antiparticle system $M = 4m_r$. As we can see this is precisely the "extra term" in Eq. (24) (assuming $P_x = K_x$ and $P_y = K_y = 0$).

If we had allowed for a general direction for the COM momentum, we would have generated both terms. So we can see that the physical origin of these terms is, in fact, the motional Stark effect; however, deriving things in this manner we have blurred the important distinction between $\mathbf{P}$ and $\mathbf{K}$, where only the latter is a conserved quantity. In what follows we will simply use Eq. (24) since it is the correct expression.

V. CENTER-OF-MASS KINETIC ENERGY SUBTRACTION

Since the energy of a particle-antiparticle state in the presence of a magnetic field has a nontrivial dependence on the pseudomomentum quantum number $\mathbf{K}$, one has to specify the precise manner in which the energy associated with the COM motion is subtracted from the total energy. Our prescription for doing this is to subtract $\langle \mathbf{P}_{\rm kinetic}\rangle^2/2M$ where $M = m_1 + m_2 = 2m_q$ from the total energy with $\langle \mathbf{P}_{\rm kinetic}\rangle$ computed via Eq. (28).

As a concrete example, let us return to the case of a harmonic interaction. As demonstrated in the previous section this can be computed analytically in the case of a harmonic interaction. Taking Eq. (38) and subtracting $\langle \mathbf{P}_{\rm kinetic}\rangle^2/2M$ with $\langle \mathbf{P}_{\rm kinetic}\rangle$ given in Eq. (43) we obtain

$$\begin{aligned}\tilde{E}_{\mathbf{K},n_\perp n_z \ell} &= E_{\mathbf{K},n_\perp n_z \ell} - \frac{\langle \mathbf{P}_{\rm kinetic}\rangle^2}{2M}, \\ &= \frac{2\omega_c^2\omega_0^2(K_x^2+K_y^2)}{M(\omega_c^2+4\omega_0^2)^2} + \left(n_z+\frac{1}{2}\right)\omega_0 \\ &\quad + (2n_\perp + 1 + |\ell|)\sqrt{\omega_0^2+\frac{\omega_c^2}{4}} - \boldsymbol{\mu}\cdot\mathbf{B} + M.\end{aligned} \tag{45}$$

As we can see from this expression, as $B \to 0$ the dependence of the COM-subtracted energy on the COM pseudomomentum vanishes as it should; however, for nonvanishing background magnetic field, there is still a residual dependence on the components of the pseudomomentum which are perpendicular to the background magnetic field. In the case of the harmonic interaction, we are able to obtain the answer analytically. In cases other than the simple harmonic interaction, it may not be possible to obtain analytic expressions. Absent analytic expressions for the energy and necessary expectation values, one must perform the subtraction prescribed in this section numerically.

VI. QUARKONIUM SPIN MIXING

Thus far we have not discussed the effects of the magnetic field-spin coupling for particle-antiparticle states. In this respect states like the J/ψ and Υ are similar to positronium (see e.g. [82,83] and references therein). We now review the mixing of the singlet and triplet states for completeness. The Hamiltonian can be written in the form

$$\hat{H} = \hat{H}_0 - \boldsymbol{\mu}\cdot\mathbf{B}, \tag{46}$$

where $\hat{H}_0$ collects all terms which depend on the spatial coordinates and

$$\begin{aligned}\boldsymbol{\mu} &= \boldsymbol{\mu}_q + \boldsymbol{\mu}_{\bar{q}} = g^-\mu_q\mathbf{S}_q + g^+\mu_q\mathbf{S}_{\bar{q}} \\ &= \frac{1}{2}g'\mu_q(\boldsymbol{\sigma}^- - \boldsymbol{\sigma}^+),\end{aligned} \tag{47}$$

where $\mu_q = Q/2m_q$ is the quark magneton and in going from the second to third lines we have used $g^- = -g^+ = g'$. Herein, we ignore effects of the anomalous magnetic moment and take $g' = 2$. The coupled spin states to be considered are

$$\begin{aligned}&|11\rangle = |\uparrow\uparrow\rangle, \quad |1{-}1\rangle = |\downarrow\downarrow\rangle, \\ &|10\rangle = \frac{1}{\sqrt{2}}(|\uparrow\downarrow\rangle + |\downarrow\uparrow\rangle), \quad |00\rangle = \frac{1}{\sqrt{2}}(|\uparrow\downarrow\rangle - |\downarrow\uparrow\rangle).\end{aligned} \tag{48}$$

In the case of $c\bar{c}$ states, the $1s$ triplet and singlet states correspond to the J/ψ and the η_c, respectively. For $b\bar{b}$ states the $1s$ triplet and singlet states correspond to the $\Upsilon(1s)$ and η_b, respectively. Without a spin-spin interaction, these states would be degenerate. With a spin-spin interaction, the triplet and singlet states split. In vacuum, the charmonium $1s$ splitting is approximately $\Delta E = 113$ MeV and for bottomonium it is approximately $\Delta E = 63$ MeV.

In the presence of a magnetic field there is mixing between some of these spin states. One can easily verify that

$$\begin{aligned}&(\sigma_z^+ - \sigma_z^-)|1\pm 1\rangle = 0, \qquad (\sigma_z^+ - \sigma_z^-)|10\rangle = 2|00\rangle, \\ &(\sigma_z^+ - \sigma_z^-)|00\rangle = 2|10\rangle.\end{aligned} \tag{49}$$

From this we see that there is no magnetic field effect on the $|1\pm 1\rangle$ spin states but there will be mixing between the $|00\rangle$ and $|10\rangle$ spin states. To determine the effect of the mixing we need only consider the two-dimensional eigensystem for the $|00\rangle$ and $|01\rangle$ states. To proceed we shift the zero of the Hamiltonian energy to the midpoint between the unperturbed singlet and triplet states and write an effective Hamiltonian of the form

$$H_{\rm eff} = \frac{\Delta E}{2}\begin{pmatrix} 1 & \chi \\ \chi & -1\end{pmatrix}, \tag{50}$$

where

$$\chi = \frac{2g'\mu_q B}{\Delta E}. \tag{51}$$

The resulting eigenstates can be expressed as

$$|\psi_\pm\rangle = \frac{1}{\sqrt{1+\varepsilon_\pm^2}}(|00\rangle + \varepsilon_\pm|10\rangle), \tag{52}$$

with $\varepsilon_\pm \equiv (1 \pm \sqrt{1+\chi^2})/\chi$. One can verify that the states are orthogonal and normalized. The energy shifts

of the states relative to the case of no spin-magnetic field effects taken into account are

$$\Delta E_{\pm} = \pm \frac{\Delta E}{2}\left(\sqrt{1+\chi^2}-1\right). \tag{53}$$

As a result, we see an increase in the energy of the $|10\rangle$ state and a decrease in the energy of the $|00\rangle$ state. In what follows we will indicate the two degenerate unmixed triplet states with a superscript $\pm$, e.g. $J/\psi^{\pm}$ and $\Upsilon^{\pm}$, and the spin-mixed triplet state with a superscript 0, e.g. J/ψ^0 and Υ^0. To close this section we note that in addition to the shifts in the energy levels, the state mixing implies that e.g. some portion of $|10\rangle$ decays will be suppressed, instead appearing as decays with an invariant mass given by the energy of the $|\psi_-\rangle$ state. This will cause suppression of e.g. Υ decays to lepton pairs and turn on decays of the η_b to lepton pairs. This would manifest itself experimentally as a reduction in dilepton yields at the Υ mass along and the appearance of a peak at the mass of the η_b. The suppression described above is similar to the experimentally well-known magnetic field suppression of the orthopositronium 3γ decays [76,77,79].

VII. HAMILTONIAN REDUCTION AND CHOICE OF POTENTIAL

In some cases, such as the case of a harmonic interaction, the energies and wave functions can be solved for analytically; however, in most cases this is not possible. In these cases it is necessary to solve the Schrödinger equation numerically. In practice, we can subtract out any terms which are independent of the position from Eq. (24). In addition, if the potential still possesses azimuthal symmetry we can set either K_x or K_y to zero by rotating the coordinate system appropriately. We choose herein to set K_y to zero. The resulting Hamiltonian which is used in the numerical solutions is then of the form

$$\mathcal{H}'_{\rm rel} = -\frac{\nabla^2}{2m_r} + \frac{qB}{4m_r}K_x y + \frac{q^2B^2}{8m_r}\rho^2 + V(\mathbf{r}). \tag{54}$$

After numerical solution using (54) the constant terms can be added back in manually in order to obtain the full energy eigenvalues.

For the charmonium and bottomonium states considered in this manuscript we use a Cornell potential plus a spin-spin interaction with a separate spin-spin potential

$$V(r) = -\frac{4}{3}\frac{\alpha_s}{r} + \sigma r + (\mathbf{S}_1\cdot\mathbf{S}_2)V_s(r). \tag{55}$$

The expectation value $\langle \mathbf{S}_1\cdot\mathbf{S}_2\rangle$ reduces to $-3/4$ for the singlet state and $1/4$ for the triplet states. For the spin potential $V_s(r)$ we use a form found from fits to the charm spin-spin potential in lattice studies [84]

$$V_s(r) = \gamma e^{-\beta r}. \tag{56}$$

For charmonia, the constants γ and β above were fit to lattice data in Ref. [84]. They found $\gamma = 0.825$ GeV and $\beta = 1.982$ GeV. In this paper we allow for variation of γ. For both charm and bottom states we will hold β fixed to the value from Ref. [84], but we adjust the amplitude γ in order to reproduce the experimentally measured splittings using Eq. (55) as the interaction potential. We present the resulting parameter sets and the corresponding $B = 0$ spectra of charmonium and bottomonium states in Appendix A. For the bottom system we present a single "tuning" which reproduces all states through the $\Upsilon(3s)$ with a maximum error of 0.22%. In the charm sector, we consider two different tunings: (a) the bottom-tuned parameter set just described (see Tables I and II in Appendix A) and (b) a charm-tuned parameter set which reproduces the masses of the $c\bar{c}$ $1s$ and $2s$ states with a maximum error of 1.3% (see Table III in Appendix A).

We note that the interaction potential and the nonderivative terms in (54) can be combined into a "pseudopotential" of the form

$$V_{\rm pseudo}(r) = \frac{qB}{4m_r}K_x y + \frac{q^2B^2}{8m_r}\rho^2 - \frac{4}{3}\frac{\alpha_s}{r} + \sigma r + (\mathbf{S}_1\cdot\mathbf{S}_2)\gamma e^{-\beta r}. \tag{57}$$

In Fig. 1(a) we plot the pseudopotential (57) as a function of y with $x = z = 0$ for charmonium states using the parameters listed in Appendix A Table II. The magnetic field amplitude is assumed to be $eB = 0.3$ GeV^2 and we take $K_x \in \{0, 2, 4, 6\}$ GeV. As can be seen from this figure, at large magnetic field magnitude it is possible for the potential to develop a nontrivial minimum which for positive K_x is at negative y. This minimum is related to the so-called motional Stark effect which was originally discussed in [46] (see [49] for a discussion in the context of positronium) and recently discussed in the context of quarkonium in Ref. [62]. As a result of this minimum, for large eB and K_x the wave function becomes bilocalized. For large enough K_x the wave function will be dominated by the leftmost minimum and the state will be "ionized" by magnetic field; however, we note that this state is, strictly speaking, not a free state since it is still confined in space by the magnetic field.

We note, for later use, that for large qB, K_x, and r, one can ignore the third and fifth terms in (57) to good approximation. Doing this and setting $x = z = 0$ one obtains

$$V_{\rm pseudo,large}{}_B(x=0,y,z=0) \simeq \frac{qB}{4m_r}K_x y + \frac{q^2B^2}{8m_r}y^2 + \sigma|y|. \tag{58}$$

We compare this approximate form to the exact pseudopotential in Fig. 1(b) for the case of charm quarks

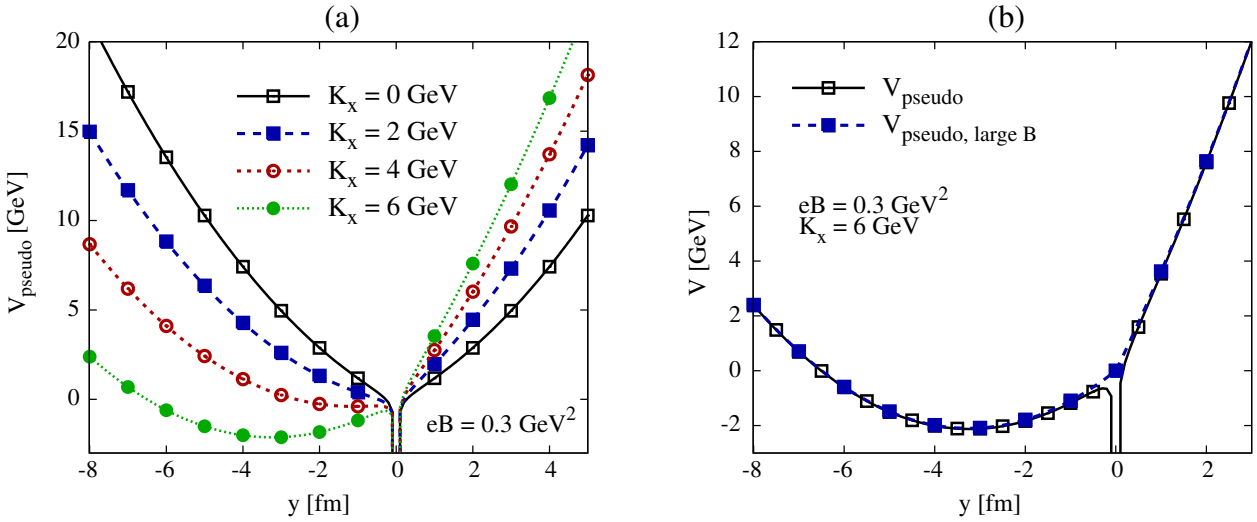

FIG. 1 (color online). (a) The pseudopotential (57) as a function of y with $x = z = 0$ for charmonium states using the parameters listed in Appendix A Table II. The magnetic field amplitude is assumed to be $eB = 0.3$ GeV^2 and we take $K_x \in \{0, 2, 4, 6\}$ GeV. (b) Comparison of the exact pseudopotential (57) with the approximate form (58) for $eB = 0.3$ GeV^2 and $K_x = 6$ GeV.

which have charge $q = 2e/3$. Based on this expression we can find the approximate location of the leftmost minimum

$$y_{\min} \simeq \frac{4\sigma m_r - qBK_x}{q^2B^2}, \tag{59}$$

from which we learn that for $qBK_x \gtrsim 4\sigma m_r$ there is a nontrivial minimum at negative y.[2] For charmonium (using the parameters listed in Appendix A Table III), this translates to the condition $eBK_x \gtrsim 0.673$ GeV^3 and for bottomonium (using the parameters listed in Appendix A Table I) $eBK_x \gtrsim 5.92$ GeV^3. For the maximum magnetic field of $eB = 0.3$ GeV^2 considered herein this translates into the constraint $K_x \gtrsim 2.24$ GeV and $K_x \gtrsim 19.7$ GeV for charmonium and bottomonium, respectively. For K_x larger than these thresholds, the state becomes bilocalized and eventually falls into the "harmonic" well. At this point the state is no longer bound by particle-anti-particle interactions, but is instead localized in space by the magnetic field.

In terms of practicalities for the numerics, we note that we use the approximate value in Eq. (59) to shift the potential along the y direction for large values K_x in order to obtain more accurate numerical results without having to resort to large volumes and/or anisotropic lattices.

VIII. RESULTS

We now present our results using the pseudopotential (57) for both charmonium and bottomonium states. For the bottomonium states, the potential parameters and resulting vacuum spectra are listed in Appendix A Table I. For charmonium states, the potential parameters and resulting vacuum spectra are listed in Appendix A Table III. The numerical algorithm used to find the eigenfunctions and eigenvalues is described in Appendix B. We note that we have tested the numerical algorithm using a harmonic interaction and have found agreement between the extracted wave functions, energy eigenvalues, etc. and the analytic formulas presented in previous sections to within machine precision. This gives us confidence in our numerical method.

A. Bottomonia

We first consider bottomonium states. In Fig. 2 we plot the masses of the 2(a) η_b, 2(b) Υ^0, and 2(c) $\Upsilon^{\pm}$ as a function of eB for $\langle P_{\text{kinetic}}\rangle \in \{0, 2, 4, 8\}$ GeV. For $\langle P_{\text{kinetic}}\rangle = 0$ GeV, we see the pattern expected, namely that the η_b mass is lowered due to spin mixing, the Υ^0 mass increases for the same reason, and the $\Upsilon^{\pm}$ states are very weakly affected (there is a small change in the mass due to the magnetic potential effects, but it is negligible). As we increase $\langle P_{\text{kinetic}}\rangle$, we see that the masses of all states increase. The result is in agreement with what we obtained analytically for the harmonic interaction [see first term in Eq. (45)]. For $\langle P_{\text{kinetic}}\rangle = 0$ and $eB = 0.3$ GeV^2 one sees a 0.06% decrease in the mass of the η_b. For $\langle P_{\text{kinetic}}\rangle = 8$ GeV, one sees an increase of 0.71% in the η_b mass. For the Υ states, the mass is a monotonically increasing function of eB and $\langle P_{\text{kinetic}}\rangle$. The maximum mass increase is on the order of 1.1% for the Υ states.

Based on the findings above one can estimate the effect of strong magnetic fields on bottomonium production in the LHC heavy ion collisions ($eB \sim 0.3$ GeV^2). The cross sections for quarkonium production from both gluon-gluon fusion and quark-antiquark annihilation both scale (to leading order) as M^{-2}. Assuming that we need only build

[2] If q is negative, the potential minimum appears at positive y instead.

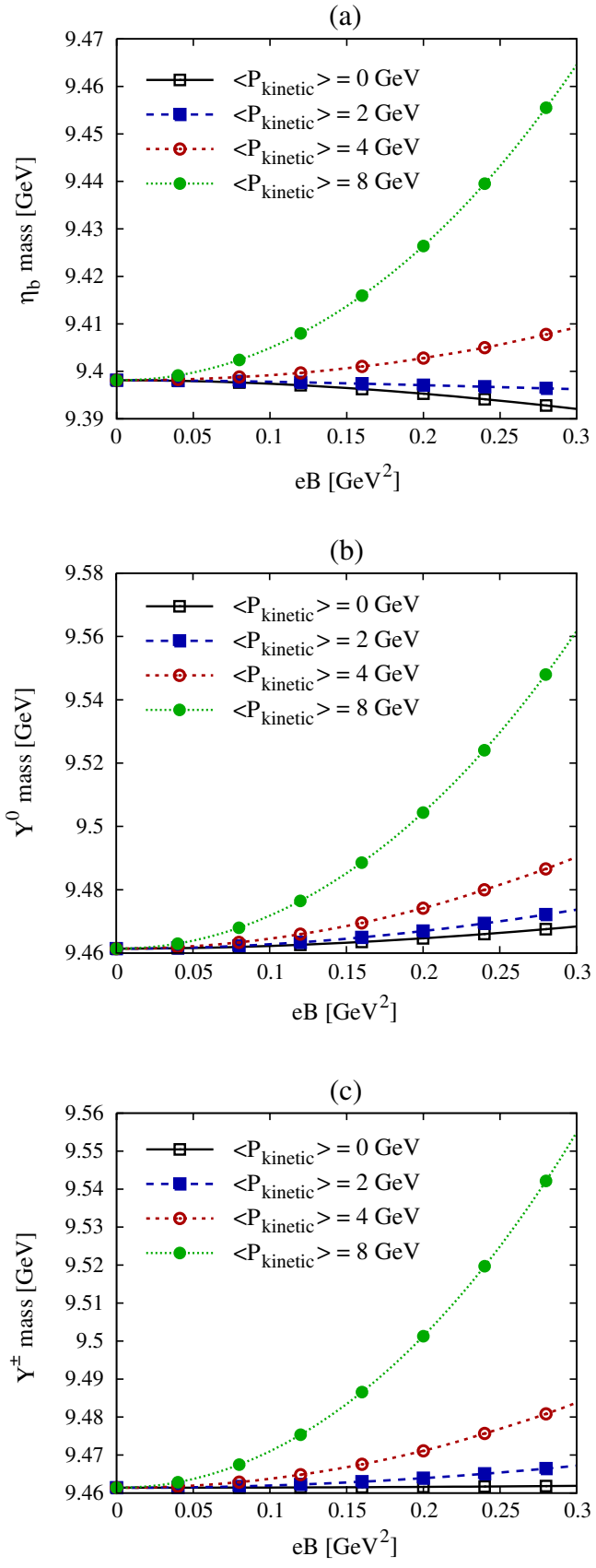

FIG. 2 (color online). Masses of the (a) η_b, (b) Υ^0, and (c) $\Upsilon^{\pm}$ as a function of eB for $\langle P_{\text{kinetic}} \rangle \in \{0, 2, 4, 8\}$ GeV.

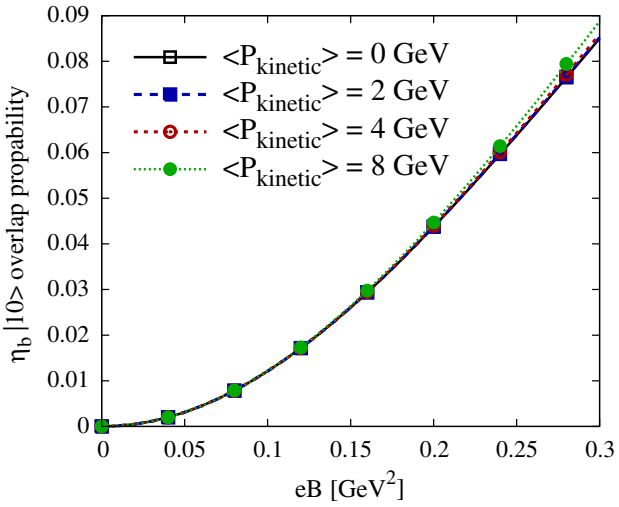

FIG. 3 (color online). Probability of finding $|10\rangle$ in the η_b state as a function of eB for $\langle P_{\text{kinetic}} \rangle \in \{0, 2, 4, 8\}$ GeV.

in the mass correction in order to account for the magnetic field, the maximal effect on $1s$ bottomonium states can be estimated to be on the order of a 2% effect.

We can extract the energy difference between the singlet and triplet states to determine the overlap probability for the $|10\rangle$ (triplet) state with, e.g. the η_b state, via Eq. (52). In vacuum, the η_b is a pure singlet state; however, a background magnetic field causes a mixing of the singlet and triplet states. In Fig. 3 we plot the η_b triplet overlap probability as a function of eB for $\langle P_{\text{kinetic}} \rangle \in \{0, 2, 4, 8\}$ GeV. As we can see from this figure, at LHC energies one estimates the overlap probability to be approximately 8.5%. This percentage of η_b states would be able to decay through dilepton decay. Correspondingly, there would be an 8.5% reduction in the dilepton decays from the Υ^0 state. The $\Upsilon^{\pm}$ states do not mix and would not have their dilepton decay rate modified. Averaging over the three different types of Υ states we would predict an approximately 2.8% suppression of $\Upsilon(1s)$ decays. The dileptons which failed to come from the Υ^0 decays, would instead appear at the mass of the η_b state. This would manifest itself through a peak in the dilepton spectrum at the η_b invariant mass. We note, however, that given finite detector resolution, it may not be possible to experimentally resolve this feature in the dilepton invariant mass spectrum. The splitting between the η_b and Υ vacuum masses is approximately 63 MeV and this is only weakly dependent on the magnetic field. The CMS and ALICE experiments have an invariant mass resolution on the order of 100 MeV [86,87] so they would not be able to see this effect, instead they would see a slight broadening of the $\Upsilon(1s)$ peak.

B. Charmonia

We now turn our attention to the charmonium states. In Fig. 4 we plot the masses of the 4(a) η_c, 4(b) J/ψ^0,

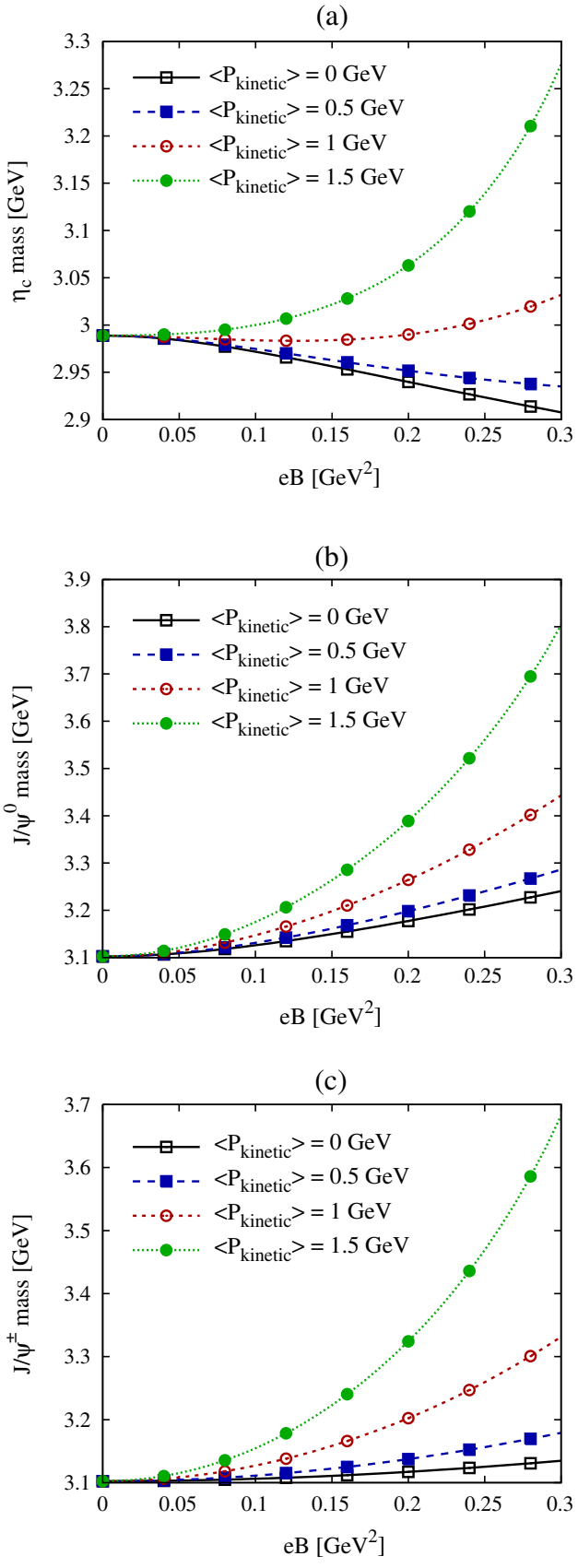

FIG. 4 (color online). Masses of the (a) η_c, (b) J/ψ^0, and (c) $J/\psi^{\pm}$ as a function of eB for $\langle P_{\text{kinetic}}\rangle \in \{0, 0.5, 1, 1.5\}$ GeV.

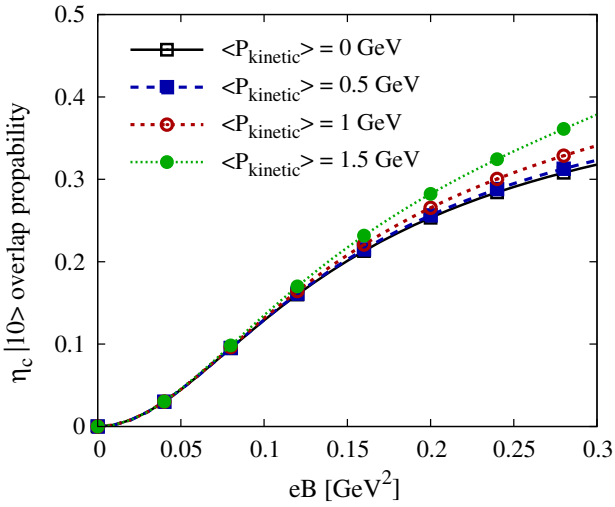

FIG. 5 (color online). Probability of finding $|10\rangle$ in the η_c state as a function of eB for $\langle P_{\text{kinetic}}\rangle \in \{0, 0.5, 1, 1.5\}$ GeV.

and 4(c) $J/\psi^{\pm}$ as a function of eB for $\langle P_{\text{kinetic}}\rangle \in \{0, 0.5, 1, 1.5\}$ GeV using the charmonium-tuned parameters listed in Appendix A Table III.[3]

For $\langle P_{\text{kinetic}}\rangle = 0$ GeV, we see the pattern expected, namely that the η_c mass is lowered due to spin mixing, the J/ψ^0 mass increases for the same reason, and the $J/\psi^{\pm}$ states are weakly affected. For $K_x = 0$ and $eB = 0.3$ GeV^2 one sees a 3.5% decrease in the mass of the η_c. For $K_x = 1.5$ GeV, one sees an increase of 19% in the η_c mass. For the J/ψ states, the mass is a monotonically increasing function of eB and $\langle P_{\text{kinetic}}\rangle$. The maximum mass increase is on the order of 31% for the J/ψ states. Again assuming that to leading order the J/ψ production cross section scales like M^{-2} one can estimate that this would result in a maximum suppression of J/ψ by approximately 42%, with the corresponding nuclear suppression being $R_{AA} \sim 0.58$.

In Fig. 5 we plot the η_c triplet overlap probability as a function of eB for $\langle P_{\text{kinetic}}\rangle \in \{0, 0.5, 1, 1.5\}$ GeV. As we can see from this figure, at LHC energies one estimates the overlap probability to be approximately 32%. This percentage of η_c states would be able to decay through dilepton decay. Correspondingly, there would be a 32% reduction in the dilepton decays from the J/ψ^0 state. The $J/\psi^{\pm}$ states do not mix and would not have their dilepton decay rate modified. Averaging over the three different types of J/ψ states we would predict an approximately 11% suppression of J/ψ decays. The dileptons which failed to come from the J/ψ^0 decays, would instead appear at the mass of the η_c state. This would manifest itself through a peak in the dilepton spectrum at the η_c invariant mass. Regarding the feasibility of measuring this effect

[3]For a comparison of the results obtained using the bottomonium-tuned potential applied to charmonium states, see Fig. 6 in Appendix A and the surrounding discussion.

experimentally, the splitting between the η_c and J/ψ vacuum masses is approximately 113 MeV and the CMS and ALICE experiments have a invariant mass resolution on the order of 30 MeV [86,87]. As a result, it may be possible to see hints of this effect in the charmonium sector. To truly confirm this effect, however, it would seem that either the detector resolution or the Crystal Ball function would need to be improved upon.

IX. CONCLUSIONS

In this paper we have made a first investigation of the effects of an external magnetic field on charmonium and bottomonium states. We have taken into account the external potential associated with the magnetic field, motional effects, and the singlet-triplet mixing of states. We solved the resulting three-dimensional Schrödinger equation analytically for the case of a harmonic interaction and numerically for a realistic quarkonium potential consisting of a Cornell potential plus a spin-spin interaction. We demonstrated that it is not possible to fully factorize the Hamiltonian of the two-particle system in the presence of the magnetic field. Instead, one can introduce a conserved quantity called the pseudomomentum, $\mathbf{K}$, which allows one to write a compact "pseudopotential" for the system which has a nontrivial dependence on the components of $\mathbf{K}$ that are perpendicular to the magnetic field. We then derived a general relation between the pseudomomentum and the kinetic COM momentum of the system. For the harmonic interaction, the latter relation could be derived analytically for all states.

Herein we have considered states with COM momentum up to 1.5 GeV in the case of $1s$ J/ψ and 10 GeV in the case of the $\Upsilon(1s)$. For J/ψ COM momentum larger than this threshold we find that the state will dissociate in the magnetic field (a similar conclusion but with a different threshold was found in Ref. [62]); however, since our results were derived in the context of a nonrelativistic limit, one expects relativistic corrections to become quantitatively important at large momenta. For this reason, it seems necessary to reformulate the problem in a relativistic framework if one wants to arrive at more reliable conclusions about the phenomenological consequences on J/ψ production. For Υ production, the threshold for magnetic field dissociation is estimated to be on the order of 20 GeV. At these high momenta, a relativistic treatment of the COM motion is necessary; however, for the range of Υ COM momenta considered herein a nonrelativistic treatment should be reasonable. Our results indicated that the maximal effect on Υ production is on the order of 2% and, as a result, it is probably safe to ignore this effect on these states. For both systems, in order to minimize the effect of magnetic fields in experimental measurements of quarkonium suppression, one can apply transverse momentum cuts which eliminate states with high COM momentum.

As part of the analysis we presented a quantitative analysis of the effect of singlet-triplet spin mixing for both charmonium and bottomonium $1s$ states. The effect causes an increase in the mass of the $|10\rangle$ triplet state and a decrease in the mass of the $|00\rangle$ state. In addition, because of the mixing, some decays of the $|10\rangle$ will appear instead at the mass of the $|00\rangle$ state; however, given the fact that the splittings in the charmonium and bottomonium states are on the order of 113 and 62 MeV, respectively, it does not seem possible to use existing experimental configurations to fully resolve this effect. With limited resolution, the mixing would appear instead as a broadening of the triplet state peak.

The estimates of the phenomenological effect of static magnetic fields obtained herein are subject to two important caveats: (1) our investigations were restricted to the vacuum Cornell potential plus a spin-spin interaction and (2) we did not investigate the effect on excited states. Regarding caveat (1), in a future study we plan to include finite-temperature effects on the potential (see e.g. [88,89]) and to simultaneously include more realistic vacuum potentials (see e.g. [90–94]). Since finite temperature effects reduce the binding energy and cause the states to be more extended in space, one can expect *a priori* that the magnetic field effect will be larger at finite temperature. Regarding caveat (2), we also plan a thorough investigation of magnetic field effects on excited states using realistic potential models. The effects on excited states are expected to be more important than on the ground state for two reasons: (a) excited states are more extended in space and are therefore more sensitive to the quadratic magnetic potential and (b) spin-mixing effects grow larger as the angular momentum representation of the state increases. Since excited state feed-down makes up on the order of 50% of both J/ψ and Υ production, one expects this to affect the ground states themselves.

Based on the two caveats laid out in the preceding paragraph, we expect that our estimates of the effect of static magnetic fields on heavy quarkonium production are a lower bound. That being said, one should also take into account the fact that the magnetic field generated in a heavy ion collision is neither static nor constant in space. One expects very strong magnetic fields only for the first 1–2 fm/c after the initial nuclear impact and as a result this would act to reduce the integrated magnetic field effect. In addition, it will be necessary to make a detailed investigation of the effect of magnetic field on the string tension and finite-temperature screened potential. We plan to investigate these effects in a future study. In closing, we have demonstrated in this paper that the effect of magnetic fields on heavy quarkonium, particularly the J/ψ, warrants further investigation. We have laid the ground work for such studies in the paper.

ACKNOWLEDGMENTS

We thank F. S. Navarra and J. Noronha for motivation and useful discussions. J. A. was supported by DOE Grant No. DE-FG02-89ER40531. M. S. was supported in part by DOE Grant No. DE-SC0004104.

APPENDIX A: POTENTIAL TUNING

In this appendix we present comparisons of bottomonium and charmonium state masses computed using the model potential (55) and experimental data [85]. We present results from the two different "tunings" which are used in the body of the manuscript separately.

1. Bottom-tuned potential

In Table I we compare bottomonia experimental data and the "bottom-tuned" potential model. The model results were computed on a lattice size of 256^3 with lattice spacing of $a = 0.1\ \mathrm{GeV}^{-1}$. The parameters used were $m_b = 4.7\ \mathrm{GeV}$, $\gamma = 0.318\ \mathrm{GeV}$, $\beta = 1.982\ \mathrm{GeV}$, $\alpha_s = 0.315443$, and $\sigma = 0.210\ \mathrm{GeV}^2$. Note that, since the potential model used herein does not include spin-orbit or tensor interactions, the model does not predict a splitting between the χ states. For these states, the error reported is computed from the average of the experimental masses.

In Table II we compare charmonia experimental data and the "bottom-tuned" potential model. The model results were computed on a lattice size of 256^3 with lattice spacing of $a = 0.2\ \mathrm{GeV}^{-1}$. The parameters used were $m_c = 1.29\ \mathrm{GeV}$, $\gamma = 0.825\ \mathrm{GeV}$, $\beta = 1.982\ \mathrm{GeV}$, $\alpha_s = 0.315443$, and $\sigma = 0.210\ \mathrm{GeV}^2$.

TABLE I. Comparison of experimentally measured particle masses from Ref. [85] for the bottomonium system with "bottom-tuned" model predictions obtained using the potential model specified in Eq. (55). The parameters used were $m_b = 4.7$ GeV, $\gamma = 0.318$ GeV, $\beta = 1.982$ GeV, $\alpha_s = 0.315443$, and $\sigma = 0.210\ \mathrm{GeV}^2$. In the case that there is no experimental data, we indicate this with three centered dots. Experiment (Exp.), Relative Error (Rel. Err.).

State	Name	Exp. [85]	Model	Rel. Err.
1^1S_0	$\eta_b(1S)$	9.398 GeV	9.398 GeV	0.001%
1^3S_1	$\Upsilon(1S)$	9.461 GeV	9.461 GeV	0.004%
1^3P_0	$\chi_{b0}(1P)$	9.859 GeV		
1^3P_1	$\chi_{b1}(1P)$	9.893 GeV	9.869 GeV	0.21%
1^3P_2	$\chi_{b2}(1P)$	9.912 GeV		
1^1P_1	$h_b(1P)$	9.899 GeV		
2^1S_0	$\eta_b(2S)$	9.999 GeV	9.977 GeV	0.22%
2^3S_1	$\Upsilon(2S)$	10.002 GeV	9.999 GeV	0.03%
2^3P_0	$\chi_{b0}(2P)$	10.232 GeV		
2^3P_1	$\chi_{b1}(2P)$	10.255 GeV	10.246 GeV	0.05%
2^3P_2	$\chi_{b2}(2P)$	10.269 GeV		
2^1P_1	$h_b(2P)$	⋯		
3^1S_0	$\eta_b(3S)$	⋯	10.344 GeV	⋯
3^3S_1	$\Upsilon(3S)$	10.355 GeV	10.358 GeV	0.03%

2. Charm-tuned potential

In Table II we present a second parameter tuning which better reproduces the energy levels of low-lying charmonium states. As can be seen from this table, even when tuned to the charmonium states, the relative errors of the heavy quark potential model spectra compared to experimental data are larger than those obtained for bottomonium states. This is to be expected and indicates that it is necessary to include relativistic corrections to obtain a more accurate reproduction of the spectrum of charmonium states. Comparing the relative errors of charmonia masses using the bottom-tuned and charm-tuned potential we expect that the charm-tuned potential is a better approximation than the bottom-tuned potential since the singlet-triplet split is very close to the experimentally determined splitting. That being said, we can use those two tunings to assess the dependence of our results on the assumed quark interaction potential. In Fig. 6 we show the scaled masses and triplet overlap probabilities using the two different tunings. In the figure, the bottom-tuned results are indicated by "BT" and the charm-tuned results by "CT." As we can see from this figure, the results obtained with the two different tunings are in qualitative agreement; however, we reiterate that we expect the charm-tuned results to be a better approximation.

TABLE II. Comparison of experimentally measured particle masses from Ref. [85] for the charmonium system with "bottom-tuned" model predictions obtained using the potential model specified in Eq. (55). The parameters used were $m_c = 1.29$ GeV, $\gamma = 0.825$ GeV, $\beta = 1.982$ GeV, $\alpha_s = 0.315443$, and $\sigma = 0.210\ \mathrm{GeV}^2$. Experiment (Exp.), Relative Error (Rel. Err.).

State	Name	Exp. [85]	Model	Rel. Error
1^1S_0	$\eta_c(1S)$	2.984 GeV	3.048 GeV	2.2%
1^3S_1	$J/\psi(1S)$	3.097 GeV	3.100 GeV	0.11%
2^1S_0	$\eta_c(2S)$	3.639 GeV	3.721 GeV	2.3%
2^3S_1	$J/\psi(2S)$	3.686 GeV	3.748 GeV	1.7%

TABLE III. Comparison of experimentally measured particle masses from Ref. [85] for the charmonium system with "charm-tuned" model predictions obtained using the potential model specified in Eq. (55). The parameters used were $m_c = 1.29$ GeV, $\gamma = 2.06$ GeV, $\beta = 1.982$ GeV, $\alpha_s = 0.234$, and $\sigma = 0.174\ \mathrm{GeV}^2$. Experiment (Exp.), Relative Error (Rel. Err.).

State	Name	Exp. [85]	Model	Rel. Error
1^1S_0	$\eta_c(1S)$	2.984 GeV	2.989 GeV	0.16%
1^3S_1	$J/\psi(1S)$	3.097 GeV	3.102 GeV	0.17%
2^1S_0	$\eta_c(2S)$	3.639 GeV	3.590 GeV	1.3%
2^3S_1	$J/\psi(2S)$	3.686 GeV	3.650 GeV	0.97%

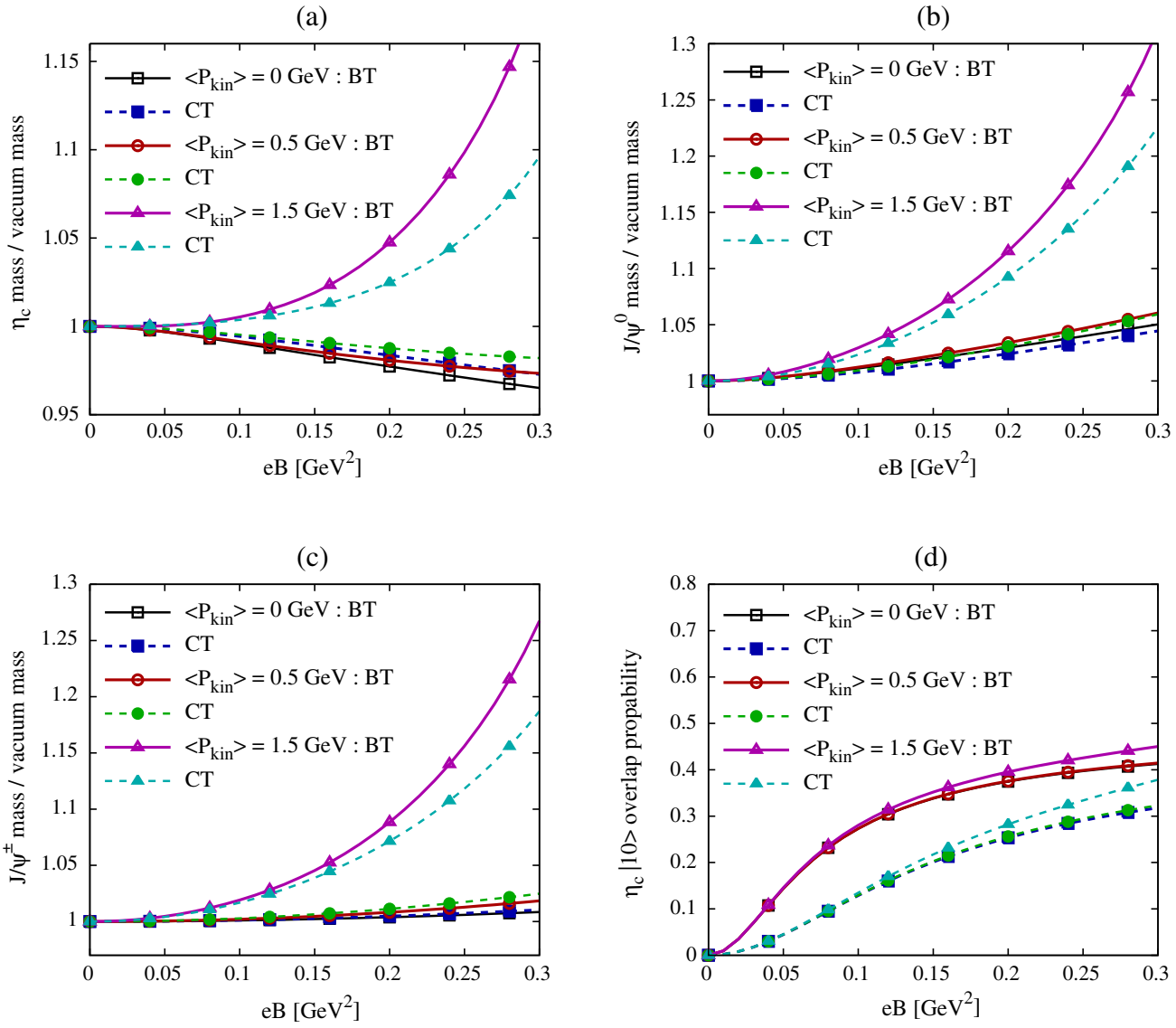

FIG. 6 (color online). Comparison of (a) η_c, (b) J/ψ^0, and (c) $J/\psi^{\pm}$ masses divided by the $eB = 0$ vacuum masses and (d) triplet overlap probability as a function of eB for $\langle P_{\text{kinetic}} \rangle \in \{0, 0.5, 1.5\}$ GeV. BT and CT indicate the results obtained using the bottom-tuned (Table II) and charm-tuned (Table III) potentials, respectively.

APPENDIX B: NUMERICAL METHOD

To solve the resulting Schrödinger equation we use the finite difference time domain method [95–97]. Here we briefly review the technique. To determine the wave functions of bound quarkonium states, we must solve the time-independent Schrödinger equation for the relative wave function

$$\hat{H}_{\text{rel}} \Psi_v(\mathbf{r}) = E_v \Psi_v(\mathbf{r}), \tag{B1}$$

on a three-dimensional lattice in coordinate space. The index v on the eigenfunctions, ϕ_v, and energies, E_v, represents a list of all relevant quantum numbers. To obtain the time-independent eigenfunctions we start with the time-dependent Schrödinger equation

$$i \frac{\partial}{\partial t} \Psi(\mathbf{x}, t) = \hat{H}_{\text{rel}} \Psi(\mathbf{x}, t), \tag{B2}$$

which can be solved by expanding in terms of the eigenfunctions, $\Psi_v(\mathbf{r})$:

$$\Psi(\mathbf{r}, t) = \sum_v c_v \Psi_v(\mathbf{r}) e^{-iE_v t}. \tag{B3}$$

If one is only interested in the lowest energy states (ground state and first few excited states) an efficient way to proceed is to transform (B2) and (B3) to Euclidean time using a Wick rotation, $\tau \equiv it$:

$$\frac{\partial}{\partial \tau} \Psi(\mathbf{r}, \tau) = -\hat{H}_{\text{rel}} \psi(\mathbf{r}, \tau), \tag{B4}$$

and

$$\Psi(\mathbf{r}, \tau) = \sum_v c_v \Psi_v(\mathbf{r}) e^{-E_v \tau}. \tag{B5}$$

For details of the discretizations used etc. we refer the reader to Ref. [96].

1. Finding the ground state

By definition, the ground state is the state with the lowest-energy eigenvalue, E_0. Therefore, at late imaginary time the sum over eigenfunctions (B5) is dominated by the ground-state eigenfunction

$$\lim_{\tau\to\infty} \Psi(\mathbf{r}, \tau) \to c_0 \Psi_0(\mathbf{r}) e^{-E_0 \tau}. \tag{B6}$$

Due to this, one can obtain the ground-state wave function, ϕ_0, and energy, E_0, by solving Eq. (B4) starting from a random three-dimensional wave function, $\Psi_{\text{initial}}(\mathbf{r}, 0)$, and evolving forward in imaginary time. The initial wave function should have a nonzero overlap with all eigenfunctions of the Hamiltonian; however, due to the damping of higher-energy eigenfunctions at sufficiently late imaginary times we are left with only the ground state, $\Psi_0(\mathbf{r})$. Once the ground-state wave function (or any other wave function) is found, we can compute its energy eigenvalue via

$$E_v(\tau \to \infty) = \frac{\langle \Psi_v | \hat{H} | \Psi_v \rangle}{\langle \Psi_v | \Psi_v \rangle} = \frac{\int d^3\mathbf{x} \Psi_v^* \hat{H} \Psi_v}{\int d^3\mathbf{x} \Psi_v^* \Psi_v}. \tag{B7}$$

2. Finding the excited states

The basic method for finding excited states is to first evolve the initially random wave function to large imaginary times, find the ground-state wave function, Ψ_0, and then project this state out from the initial wave function and reevolve the partial-differential equation in imaginary time. However, there are (at least) two more efficient ways to accomplish this. The first is to record snapshots of the 3D wave function at a specified interval τ_{snapshot} during a single evolution in τ. After having obtained the ground-state wave function, one can go back and extract the excited states by projecting out the ground-state wave function from the recorded snapshots of $\Psi(\mathbf{r}, \tau)$ [95,96].

An alternative way to select different excited states is to impose a symmetry condition on the initially random wave function which cannot be broken by the Hamiltonian evolution [96]. For example, one can select the first p-wave excited state by antisymmetrizing the initial wave function around either the x, y, or z axes. In the nonspherical case this method can be used to separate the different excited state polarizations in the quarkonium system and to determine their energy eigenvalues with high precision.

APPENDIX C: APPLICATION OF THE SUDDEN APPROXIMATION

In this appendix we explore what happens to a system which suddenly has a magnetic field turned on. We will model this as being instantaneous in order to simplify the treatment and restrict our attention to a linear combination of 3D harmonic oscillator eigenstates since it is possible to make much more analytic progress in this case. We start by positing that for $t < 0$ there is no magnetic field and that the system is subject only to an internal harmonic interaction in which case the full state can be decomposed in terms of the no-magnetic-field eigenstates $\Phi_k^{(0)}$

$$\Phi(t) = \sum_k c_k \Phi_k^{(0)} e^{-iE_k^{(0)} t} \qquad t < 0, \tag{C1}$$

where k collects all relevant quantum numbers and the sum represents a sum over discrete quantum numbers and integral for continuous quantum numbers. For $t \geq 0$ we can expand in terms of the eigenstates in the presence of the magnetic field $\Phi_m^{(1)}$

$$\Phi(t) = \sum_m d_m \Phi_m^{(1)} e^{-iE_m^{(1)} t} \qquad t \geq 0. \tag{C2}$$

At $t = 0$ we match the coefficients which requires

$$d_n = \sum_k c_k \langle \Phi_n^{(1)} \mid \Phi_k^{(0)} \rangle. \tag{C3}$$

1. Pure state for $t < 0$

If the state for $t < 0$ is a pure state with $c_k = \delta_{km}$ we obtain $d_n = \langle \Phi_n^{(1)} \mid \Phi_m^{(0)} \rangle$. We now turn to the computation of the overlap integrals necessary for the case at hand. The $t < 0$ states are

$$\Phi^{(0)}_{\mathbf{P}, n_\perp^0 n_z^0 \ell^0}(\mathbf{R}, \mathbf{r}) = \mathcal{N}^{(0)} \rho^{|\ell^0|} e^{i\ell^0\phi} e^{-\frac{1}{2}\gamma^2(\rho^2+z^2)} \times H_{n_z^0}(\gamma z) L_{n_\perp^0}^{|\ell^0|}(\gamma^2\rho^2) e^{i\mathbf{P}\cdot\mathbf{R}}, \tag{C4}$$

where

$$\mathcal{N}^{(0)} = \frac{\gamma^{|\ell^0|+3/2}}{\sqrt{2^{n_z^0}\pi^{3/2}}} \sqrt{\frac{n_\perp^0!}{n_z^0!(|\ell^0|+n_\perp^0)!}}, \tag{C5}$$

and the $t \geq 0$ states are

$$\Phi^{(1)}_{\mathbf{K}, n_\perp n_z \ell}(\mathbf{R}, \mathbf{r}) = \mathcal{N}^{(1)} \tilde{\rho}^{|\ell|} e^{i\ell\tilde{\phi}} e^{-\frac{1}{2}\gamma^2 z^2} e^{-\frac{1}{2}\alpha^2\tilde{\rho}^2} H_{n_z}(\gamma z) \times L_{n_\perp}^{|\ell|}(\alpha^2\tilde{\rho}^2) e^{i(\mathbf{K} - \frac{1}{2}q\mathbf{B}\times\mathbf{r})\cdot\mathbf{R}}, \tag{C6}$$

with

$$\omega_c = \frac{qB}{m_r}, \qquad \alpha^2 = m_r\sqrt{\omega_0^2 + \frac{\omega_c^2}{4}},$$
$$\gamma^2 = m_r\omega_0, \qquad \tilde{\rho}^2 = (x - \lambda K_y)^2 + (y + \lambda K_x)^2, \tag{C7}$$
$$\tilde{\phi} = \arctan\left(\frac{y + \lambda K_x}{x - \lambda K_y}\right), \qquad \lambda = \frac{\omega_c}{4m_r(\omega_0^2 + \omega_c^2/4)},$$

and

$$\mathcal{N}^{(1)} = \frac{\alpha^{|\ell|+1}\gamma^{1/2}}{\sqrt{2^{n_z}\pi^{3/2}}}\sqrt{\frac{n_\perp!}{n_z!(|\ell|+n_\perp)!}}. \tag{C8}$$

The six-dimensional overlap integral in relative cylindrical coordinates becomes

$$\begin{aligned} d_n = {} & \mathcal{N}^{(0)}\mathcal{N}^{(1)}\int_0^\infty \rho d\rho \int_0^{2\pi} d\phi \int_{-\infty}^{\infty} dz \\ & \times \int d^3\mathbf{R}\,\rho^{|\ell^0|}\tilde{\rho}^{|\ell|}e^{i(\ell^0\phi-\ell\tilde{\phi})}e^{-\gamma^2 z^2}e^{-\frac{1}{2}(\gamma^2\rho^2+\alpha^2\tilde{\rho}^2)} \\ & \times H_{n_z}(\gamma z)H_{n_z^0}(\gamma z)L_{n_\perp^0}^{|\ell^0|}(\gamma^2\rho^2) \\ & \times L_{n_\perp}^{|\ell|}(\alpha^2\tilde{\rho}^2)e^{i(\mathbf{P}-\mathbf{K}+\frac{1}{2}q\mathbf{B}\times\mathbf{r})\cdot\mathbf{R}}. \end{aligned} \tag{C9}$$

Using $\frac{1}{2}q\mathbf{B}\times\mathbf{r} = \frac{1}{2}qB(-y,x,0) = \frac{1}{2}qB\rho(-\sin\phi,\cos\phi,0)$ and the orthonormality of the Hermite polynomials we can perform the z and $\mathbf{Z}$ integrations. Using the exponential we can further perform the $\mathbf{X}$ and $\mathbf{Y}$ integrations. The remaining two integrals are evaluated in Cartesian coordinates. The result is

$$\begin{aligned} d_n = {} & \tilde{\mathcal{N}}_{nm}\left(\frac{2}{|q|B}\right)^2\delta_{n_z n_z^0}\delta(P_z-K_z)\rho^{|\ell^0|}\tilde{\rho}^{|\ell|}e^{i(\ell^0\phi-\ell\tilde{\phi})} \\ & \times e^{-\frac{1}{2}(\gamma^2\rho^2+\alpha^2\tilde{\rho}^2)}L_{n_\perp^0}^{|\ell^0|}(\gamma^2\rho^2)L_{n_\perp}^{|\ell|}(\alpha^2\tilde{\rho}^2), \end{aligned} \tag{C10}$$

where

$$\begin{aligned} \tilde{\mathcal{N}}_{nm} &= (2\pi)^3\mathcal{N}^{(0)}\mathcal{N}^{(1)}\sqrt{\pi}2^{n_z}n_z!/\gamma \\ &= 2(2\pi)^2\alpha^{|\ell|+1}\gamma^{|\ell^0|+1}\sqrt{\frac{n_\perp^0!n_\perp!}{(|\ell^0|+n_\perp^0)!(|\ell|+n_\perp)!}}, \\ \rho^2 &= x^2+y^2 = \left(\frac{2}{qB}\right)^2[(P_x-K_x)^2+(P_y-K_y)^2], \\ \phi &= \arctan\left(\frac{y}{x}\right) = \arctan\left(\frac{P_x-K_x}{K_y-P_y}\right), \\ \tilde{\rho}^2 &= \left(\frac{2}{qB}\right)^2[(\beta K_y-P_y)^2+(P_x-\beta K_x)^2], \\ \tilde{\phi} &= \arctan\left(\frac{P_x-\beta K_x}{\beta K_y-P_y}\right), \end{aligned} \tag{C11}$$

with $\beta \equiv (8\omega_0^2+\omega_c^2)/(8\omega_0^2+2\omega_c^2)$, which satisfies $\frac{1}{2} \le \beta \le 1$. Note that the above definitions only apply for the probability amplitude d_n. For $\tilde{\rho}$ and $\tilde{\phi}$ in the wave function, we need to use the definitions in Eq. (C7).

2. Gaussian wave packet as initial condition

Let us consider that the initial condition is not a pure state but instead a Gaussian linear combination

$$\Phi(t) = \sum_k c_k\Phi_k^{(0)}e^{-iE_k^{(0)}t}, \tag{C12}$$

where $k = (\ell, k_z, k_\perp, \mathbf{P})$. We will assume that the system is in a well-defined internal state $(\ell^0, n_z^0, n_\perp^0)$ but has a spread in COM momentum:

$$c_k = \sqrt{\frac{8\pi^{3/2}}{\sigma^3}}\delta_{\ell^0\ell}\delta_{n_z^0 k_z}\delta_{n_\perp^0 k_\perp}e^{-(\mathbf{P}-\mathbf{P}^0)^2/(2\sigma^2)}. \tag{C13}$$

In this case the coefficient d_n is more complicated, $d_n = \sum_m c_m\langle\Phi_n^{(1)}\mid\Phi_m^{(0)}\rangle$; however, we can use the pure state result obtained previously

$$\begin{aligned} \langle\Phi_n^{(1)}\mid\Phi_m^{(0)}\rangle = {} & \tilde{\mathcal{N}}_{nm}\left(\frac{2}{|q|B}\right)^2\delta_{n_z n_z^0}\delta(P_z-K_z) \\ & \times \rho^{|\ell^0|}\tilde{\rho}^{|\ell|}e^{i(\ell^0\phi-\ell\tilde{\phi})}e^{-\frac{1}{2}(\gamma^2\rho^2+\alpha^2\tilde{\rho}^2)} \\ & \times L_{n_\perp^0}^{|\ell^0|}(\gamma^2\rho^2)L_{n_\perp}^{|\ell|}(\alpha^2\tilde{\rho}^2), \end{aligned} \tag{C14}$$

with $m = (\ell^0, n_z^0, n_\perp^0, \mathbf{P})$ and $n = (\ell, n_z, n_\perp, \mathbf{K})$.

3. Time evolution of the center-of-mass kinetic momentum

We consider next the evolution of the COM kinetic momentum after the magnetic field is applied. We seek to evaluate $\langle\mathbf{P}_{\text{kinetic}}\rangle = \langle\Phi(t)|\mathbf{P}_{\text{kinetic}}|\Phi(t)\rangle$ for $t > 0$,

$$\begin{aligned} & \langle\Phi(t)|\mathbf{P}_{\text{kinetic}}|\Phi(t)\rangle \\ & \quad = \sum_{m,n} d_m^* d_n\langle\Phi_m^{(1)}|\mathbf{P}_{\text{kinetic}}|\Phi_n^{(1)}\rangle e^{-i(E_n^{(1)}-E_m^{(1)})t}, \end{aligned} \tag{C15}$$

where $m = (\ell', n_z', n_\perp', \mathbf{K}')$, $n = (\ell, n_z, n_\perp, \mathbf{K})$, and

$$\begin{aligned} \sum_m &\equiv \sum_{n_z'=0}^{\infty}\sum_{\ell'=-\infty}^{\infty}\sum_{n_\perp'=0}^{\infty}\int\frac{d^3\mathbf{K}'}{(2\pi)^3}, \\ \sum_n &\equiv \sum_{n_z=0}^{\infty}\sum_{\ell=-\infty}^{\infty}\sum_{n_\perp=0}^{\infty}\int\frac{d^3\mathbf{K}}{(2\pi)^3}, \end{aligned} \tag{C16}$$

$$\begin{aligned} \langle\Phi_m^{(1)}|\mathbf{P}_{\text{kinetic}}|\Phi_n^{(1)}\rangle &= \langle\Phi_m^{(1)}|\mathbf{K}-q\mathbf{B}\times\mathbf{r}|\Phi_n^{(1)}\rangle \\ &= \mathbf{K}\delta_{mn} - qB\langle\Phi_m^{(1)}\Big|\Big(-\tilde{\rho}\sin\tilde{\phi} \\ &\quad + \frac{c}{a}, \tilde{\rho}\cos\tilde{\phi}+\frac{b}{a}, 0\Big)\Big|\Phi_n^{(1)}\rangle, \end{aligned} \tag{C17}$$

where $\delta_{mn} = \delta_{\ell'\ell}\delta_{n_z' n_z}\delta_{n_\perp' n_\perp}\delta_{\mathbf{K}'\mathbf{K}}$, $\delta_{\mathbf{K}'\mathbf{K}} \equiv (2\pi)^3\delta^3\times(\mathbf{K}'-\mathbf{K})$, and we remind the reader that $a = m_r(\omega_0^2+\omega_c^2/4)$, $b = \omega_c K_y/4$, $c = \omega_c K_x/4$. Considering the second term we have

$$\begin{aligned} & \Big(-\langle\Phi_m^{(1)}|\tilde{\rho}\sin\tilde{\phi}|\Phi_n^{(1)}\rangle \\ & \quad + \frac{c}{a}\delta_{mn},\langle\Phi_m^{(1)}|\tilde{\rho}\cos\tilde{\phi}|\Phi_n^{(1)}\rangle + \frac{b}{a}\delta_{mn}, 0\Big). \end{aligned} \tag{C18}$$

To proceed, we first consider $J_{mn}^+ \equiv \langle\Phi_m^{(1)}|\tilde{\rho}e^{i\tilde{\phi}}|\Phi_n^{(1)}\rangle$ and $J_{mn}^- \equiv \langle\Phi_m^{(1)}|\tilde{\rho}e^{-i\tilde{\phi}}|\Phi_n^{(1)}\rangle$. For $\ell \ge 0$,

$$\begin{aligned} J_{mn}^+ = {} & \frac{\delta_{\mathbf{K}'\mathbf{K}}\delta_{n_z' n_z}\delta_{\ell',\ell+1}}{\alpha} \\ & \times\Big[\delta_{n_\perp' n_\perp}\sqrt{n_\perp+\ell+1} - \delta_{n_\perp',n_\perp-1}\sqrt{n_\perp}\Big]. \end{aligned} \tag{C19}$$

For $\ell \leq -1$,

$$J^{+}_{mn} = \frac{\delta_{\mathbf{K}'\mathbf{K}}\delta_{n'_z n_z}\delta_{\ell',\ell+1}}{\alpha} \times \Big[\delta_{n'_\perp n_\perp}\sqrt{n_\perp - \ell} - \delta_{n'_\perp, n_\perp+1}\sqrt{n_\perp + 1}\Big]. \quad \text{(C20)}$$

For $\ell \geq 1$,

$$J^{-}_{mn} = \frac{\delta_{\mathbf{K}'\mathbf{K}}\delta_{n'_z n_z}\delta_{\ell',\ell-1}}{\alpha} \times \Big[\delta_{n'_\perp n_\perp}\sqrt{n_\perp + \ell} - \delta_{n'_\perp, n_\perp+1}\sqrt{n_\perp + 1}\Big]. \quad \text{(C21)}$$

For $\ell \leq 0$,

$$J^{-}_{mn} = \frac{\delta_{\mathbf{K}'\mathbf{K}}\delta_{n'_z n_z}\delta_{\ell',\ell-1}}{\alpha} \times \Big[\delta_{n'_\perp n_\perp}\sqrt{n_\perp - \ell + 1} - \delta_{n'_\perp, n_\perp-1}\sqrt{n_\perp}\Big]. \quad \text{(C22)}$$

With these we have determined

$$\begin{aligned}\langle \Phi^{(1)}_m|\tilde{\rho}\sin\tilde{\phi}|\Phi^{(1)}_n\rangle &= \frac{1}{2i}(J^{+}_{mn} - J^{-}_{mn}) \equiv \mathcal{S}_{mn},\\ \langle \Phi^{(1)}_m|\tilde{\rho}\cos\tilde{\phi}|\Phi^{(1)}_n\rangle &= \frac{1}{2}(J^{+}_{mn} + J^{-}_{mn}) \equiv \mathcal{C}_{mn}.\end{aligned} \quad \text{(C23)}$$

To evaluate $\langle\Phi(t)|\mathbf{P}_{\rm kinetic}|\Phi(t)\rangle$ we will need

$$\begin{aligned}&\sum_{\ell=-\infty}^{\infty}\sum_{n_\perp=0}^{\infty}\sum_{\ell'=-\infty}^{\infty}\sum_{n'_\perp=0}^{\infty}\int_{\mathbf{K}'} d^*_m d_n J^{\pm}_{mn} e^{-i(E^{(1)}_n - E^{(1)}_m)t}\\ &= \frac{1}{\alpha}\sum_{\ell=0}^{\infty}\sum_{n_\perp=0}^{\infty}\Big[d^*_{\pm(\ell+1),n_\perp} d_{\pm\ell,n_\perp}\sqrt{n_\perp+\ell+1}\,e^{i\alpha^2 t/m_r}\\ &\quad - d^*_{\pm(\ell+1),n_\perp-1} d_{\pm\ell,n_\perp}\sqrt{n_\perp}\,e^{-i\alpha^2 t/m_r}\Big]\\ &\quad + \frac{1}{\alpha}\sum_{\ell=1}^{\infty}\sum_{n_\perp=0}^{\infty}\Big[d^*_{\mp(\ell-1),n_\perp} d_{\mp\ell,n_\perp}\sqrt{n_\perp+\ell}\,e^{-i\alpha^2 t/m_r}\\ &\quad - d^*_{\mp(\ell-1),n_\perp+1} d_{\mp\ell,n_\perp}\sqrt{n_\perp+1}\,e^{i\alpha^2 t/m_r}\Big],\end{aligned} \quad \text{(C24)}$$

where we have used Eq. (38).

To proceed we note that $d^*_{\ell,n_\perp} d_{\ell',n'_\perp} = d^*_{-\ell',n'_\perp} d_{-\ell,n_\perp}$. Now we have after some work

$$\begin{aligned}&\sum_{\ell=-\infty}^{\infty}\sum_{n_\perp=0}^{\infty}\sum_{\ell'=-\infty}^{\infty}\sum_{n'_\perp=0}^{\infty}\int_{\mathbf{K}'} d^*_m d_n (J^{+}_{mn} \pm J^{-}_{mn}) e^{-i(E^{(1)}_n - E^{(1)}_m)t}\\ &= \frac{2}{\alpha}\sum_{\ell=0}^{\infty}\sum_{n_\perp=0}^{\infty}\Big[(d^*_{-\ell,n_\perp} d_{-\ell-1,n_\perp} \pm d^*_{\ell,n_\perp} d_{\ell+1,n_\perp})\\ &\quad \times\sqrt{n_\perp+\ell+1} - (d^*_{-\ell,n_\perp+1} d_{-\ell-1,n_\perp}\\ &\quad \pm d^*_{\ell,n_\perp+1} d_{\ell+1,n_\perp})\sqrt{n_\perp+1}\Big]\cos(\alpha^2 t/m_r).\end{aligned} \quad \text{(C25)}$$

Using $d_{\ell,n_\perp} = \int d^2\mathbf{P}_\perp m_{\ell,n_\perp}$ with

$$\begin{aligned}m_{\ell,n_\perp} &= \frac{\tilde{\mathcal{N}}}{(2\pi)^3}\sqrt{\frac{8\pi^{3/2}}{\sigma^3}}\Big(\frac{2}{|q|B}\Big)^2 \delta_{n^0_z n_z} e^{-(K_z - P^0_z)^2/(2\sigma^2)}\\ &\quad\times e^{-(\mathbf{P}_\perp - \mathbf{P}^0_\perp)^2/(2\sigma^2)}\rho^{|\ell^0|}\tilde{\rho}^{|\ell|} e^{i(\ell^0\phi - \ell\tilde{\phi})} e^{-\frac{1}{2}(\gamma^2\rho^2 + \alpha^2\tilde{\rho}^2)}\\ &\quad\times L^{|\ell^0|}_{n^0_\perp}(\gamma^2\rho^2) L^{|\ell|}_{n_\perp}(\alpha^2\tilde{\rho}^2),\end{aligned} \quad \text{(C26)}$$

$$\tilde{\mathcal{N}} = 2(2\pi)^2\alpha^{|\ell|+1}\gamma^{|\ell^0|+1}\sqrt{\frac{n^0_\perp!\,n_\perp!}{(|\ell^0| + n^0_\perp)!(|\ell| + n_\perp)!}}, \quad \text{(C27)}$$

and a recurrence relation for the Laguerre polynomials one obtains in the end

$$\begin{aligned}\langle\mathbf{P}_{\rm kinetic}\rangle &= \sum_{n_z=0}^{\infty}\sum_{n_\perp=0}^{\infty}\sum_{\ell=-\infty}^{\infty}\int\frac{d^3\mathbf{K}}{(2\pi)^3} d^*_n d_n\Big[\mathbf{K} - qB\Big(\frac{c}{a},\frac{b}{a},0\Big)\Big]\\ &\quad - 2qB\cos(\alpha^2 t/m_r)\sum_{n_z=0}^{\infty}\sum_{n_\perp=0}^{\infty}\sum_{\ell=0}^{\infty}\int\frac{d^3\mathbf{K}}{(2\pi)^3} d^*_{\ell,n_\perp}\\ &\quad\times\int d^2\mathbf{P}_\perp m_{\ell,n_\perp}\tilde{\rho}(-\sin\tilde{\phi},\cos\tilde{\phi},0).\end{aligned} \quad \text{(C28)}$$

Focusing on the second term, we need to evaluate

$$\sum_{n_z=0}^{\infty}\sum_{n_\perp=0}^{\infty}\sum_{\ell=0}^{\infty}\int\frac{d^3\mathbf{K}}{(2\pi)^3} d^*_{\ell,n_\perp}\int d^2\mathbf{P}_\perp m_{\ell,n_\perp}\tilde{\rho}(-\sin\tilde{\phi},\cos\tilde{\phi},0). \quad \text{(C29)}$$

The summation over n_z and integration over K_z can be done analytically. Next, we change integration variables from $(\mathbf{K}_\perp, \mathbf{P}_\perp)$ to $(\rho, \phi, \tilde{\rho}, \tilde{\phi})$ and use the completeness of the Laguerre polynomials to eliminate the summation over $n_\perp$. Now, one of the integrals over $\tilde{\rho}$ and the summation over ℓ can be done analytically. The remaining five integrals are evaluated numerically and found to converge to zero. We now have

$$\begin{aligned}\langle\mathbf{P}_{\rm kinetic}\rangle &= \sum_{n_z=0}^{\infty}\sum_{n_\perp=0}^{\infty}\sum_{\ell=-\infty}^{\infty}\int\frac{d^3\mathbf{K}}{(2\pi)^3} d^*_n d_n\Big[\mathbf{K} - qB\Big(\frac{c}{a},\frac{b}{a},0\Big)\Big]\\ &= \frac{4\omega_0^2}{4\omega_0^2 + \omega_c^2}\sum_{n_z=0}^{\infty}\sum_{n_\perp=0}^{\infty}\sum_{\ell=-\infty}^{\infty}\int\frac{d^3\mathbf{K}}{(2\pi)^3} d^*_n d_n \mathbf{K}_\perp\\ &\quad + \hat{z}\sum_{n_z=0}^{\infty}\sum_{n_\perp=0}^{\infty}\sum_{\ell=-\infty}^{\infty}\int\frac{d^3\mathbf{K}}{(2\pi)^3} d^*_n d_n K_z.\end{aligned} \quad \text{(C30)}$$

Again, the summation over n_z and integration over K_z can be done analytically. We change variables, use the completeness of the Laguerre polynomials, and do one of the integrals over $\tilde{\rho}$. Now, we use the completeness of the azimuthal modes and do one of the integrals over $\tilde{\phi}$,

$$\langle \mathbf{P}_{\text{kinetic}} \rangle = \left(\frac{\lambda}{\pi\sigma}\right)^2 \gamma^{2(|\ell^0|+1)} \frac{4\omega_0^2}{4\omega_0^2+\omega_c^2} \frac{n_\perp^0!}{(|\ell^0|+n_\perp^0)!} \int \rho d\rho \int d\phi \rho^{2|\ell^0|} e^{-\gamma^2\rho^2} (L_{n_\perp^0}^{|\ell^0|}(\gamma^2\rho^2))^2 \int \tilde{\rho} d\tilde{\rho} \int d\tilde{\phi} \mathbf{K}_\perp e^{-(\mathbf{P}_\perp - \mathbf{P}_\perp^0)^2/\sigma^2}$$
$$+ \hat{z} \left(\frac{\lambda}{\pi\sigma}\right)^2 \gamma^{2(|\ell^0|+1)} P_z^0 \frac{n_\perp^0!}{(|\ell^0|+n_\perp^0)!} \int \rho d\rho \int d\phi \rho^{2|\ell^0|} e^{-\gamma^2\rho^2} (L_{n_\perp^0}^{|\ell^0|}(\gamma^2\rho^2))^2 \int \tilde{\rho} d\tilde{\rho} \int d\tilde{\phi} e^{-(\mathbf{P}_\perp - \mathbf{P}_\perp^0)^2/\sigma^2}. \tag{C31}$$

Using $P_x = -\lambda(\beta y - \tilde{y})$, $P_y = \lambda(\beta x - \tilde{x})$, $K_x = -\lambda(y - \tilde{y})$, $K_y = \lambda(x - \tilde{x})$, and the orthogonality of the Laguerre polynomials, the remaining integrals can be done analytically. The final result is

$$\langle \mathbf{P}_{\text{kinetic}} \rangle = \left(\frac{4\omega_0^2}{4\omega_0^2+\omega_c^2} P_x^0, \frac{4\omega_0^2}{4\omega_0^2+\omega_c^2} P_y^0, P_z^0 \right). \tag{C32}$$

[1] P. Zeeman, Philos. Mag. **43**, 226 (1897).
[2] P. Zeeman, Philos. Mag. **44**, 55 (1897).
[3] P. Zeeman, Nature (London) **55**, 347 (1897).
[4] K. Fukushima, D. E. Kharzeev, and H. J. Warringa, Phys. Rev. D **78**, 074033 (2008).
[5] V. Skokov, A. Y. Illarionov, and V. Toneev, Int. J. Mod. Phys. A **24**, 5925 (2009).
[6] K. Fukushima, D. E. Kharzeev, and H. J. Warringa, Phys. Rev. Lett. **104**, 212001 (2010).
[7] V. Voronyuk, V. D. Toneev, W. Cassing, E. L. Bratkovskaya, V. P. Konchakovski, and S. A. Voloshin, Phys. Rev. C **83**, 054911 (2011).
[8] W.-T. Deng and X.-G. Huang, Phys. Rev. C **85**, 044907 (2012).
[9] K. Tuchin, Adv. High Energy Phys. **2013**, 490495 (2013).
[10] R. C. Duncan and C. Thompson, Astrophys. J. Lett. **392**, L9 (1992).
[11] D. T. Son and N. Yamamoto, Phys. Rev. Lett. **109**, 181602 (2012).
[12] J.-W. Chen, S. Pu, Q. Wang, and X.-N. Wang, Phys. Rev. Lett. **110**, 262301 (2013).
[13] M. D'Elia, S. Mukherjee, and F. Sanfilippo, Phys. Rev. D **82**, 051501 (2010).
[14] M. D'Elia and F. Negro, Phys. Rev. D **83**, 114028 (2011).
[15] G. S. Bali, F. Bruckmann, G. Endrődi, Z. Fodor, S. D. Katz, S. Krieg, A. Schäfer, and K. K. Szabó, J. High Energy Phys. 02 (2012) 044.
[16] G. S. Bali, F. Bruckmann, G. Endrődi, Z. Fodor, S. D. Katz, and A. Schäfer, Phys. Rev. D **86**, 071502 (2012).
[17] G. Bali, F. Bruckmann, G. Endrődi, F. Gruber, and A. Schaefer, J. High Energy Phys. 04 (2013) 130.
[18] J. Alexandre, Phys. Rev. D **63**, 073010 (2001).
[19] N. Agasian and S. Fedorov, Phys. Lett. B **663**, 445 (2008).
[20] E. S. Fraga and A. J. Mizher, Phys. Rev. D **78**, 025016 (2008).
[21] A. J. Mizher, M. Chernodub, and E. S. Fraga, Phys. Rev. D **82**, 105016 (2010).
[22] K. Fukushima, M. Ruggieri, and R. Gatto, Phys. Rev. D **81**, 114031 (2010).
[23] R. Gatto and M. Ruggieri, Phys. Rev. D **82**, 054027 (2010).
[24] R. Gatto and M. Ruggieri, Phys. Rev. D **83**, 034016 (2011).
[25] F. Preis, A. Rebhan, and A. Schmitt, J. High Energy Phys. 03 (2011) 033.
[26] F. Preis, A. Rebhan, and A. Schmitt, J. Phys. G **39**, 054006 (2012).
[27] J. O. Andersen and R. Khan, Phys. Rev. D **85**, 065026 (2012).
[28] J. Erdmenger, V. G. Filev, and D. Zoakos, J. High Energy Phys. 08 (2012) 004.
[29] E. Gorbar, V. Miransky, and I. Shovkovy, Prog. Part. Nucl. Phys. **67**, 547 (2012).
[30] V. Skokov, Phys. Rev. D **85**, 034026 (2012).
[31] K. Kashiwa, Phys. Rev. D **83**, 117901 (2011).
[32] E. S. Fraga and L. F. Palhares, Phys. Rev. D **86**, 016008 (2012).
[33] E. S. Fraga, J. Noronha, and L. F. Palhares, Phys. Rev. D **87**, 114014 (2013).
[34] E. S. Fraga, Lect. Notes Phys. **871**, 121 (2013).
[35] J. O. Andersen, Phys. Rev. D **86**, 025020 (2012).
[36] I. A. Shovkovy, Lect. Notes Phys. **871**, 13 (2013).
[37] F. Preis, A. Rebhan, and A. Schmitt, Lect. Notes Phys. **871**, 51 (2013).
[38] G. N. Ferrari, A. F. Garcia, and M. B. Pinto, Phys. Rev. D **86**, 096005 (2012).
[39] S. Fayazbakhsh, S. Sadeghian, and N. Sadooghi, Phys. Rev. D **86**, 085042 (2012).
[40] K. Fukushima and J. M. Pawlowski, Phys. Rev. D **86**, 076013 (2012).
[41] M. de Paoli and D. Menezes, arXiv:1203.3175.
[42] T. Kojo and N. Su, Phys. Lett. B **720**, 192 (2013).
[43] T. Kojo and N. Su, Phys. Lett. B **726**, 839 (2013).
[44] W. E. Lamb and R. C. Retherford, Phys. Rev. **79**, 549 (1950).
[45] W. E. Lamb and R. C. Retherford, Phys. Rev. **81**, 222 (1951).
[46] W. E. Lamb, Phys. Rev. **85**, 259 (1952).
[47] B. P. Carter, Lawrence Radiation Laboratory Report No. UCID-15180 1967.
[48] L. P. Gor'kov and I. E. Dzyaloshinskii, Sov. Phys. JETP **63**, 449 (1968).
[49] H. Grotch and R. A. Hegstrom, Phys. Rev. A **4**, 59 (1971).
[50] J. Avron, I. Herbst, and B. Simon, Ann. Phys. (N.Y.) **114**, 431 (1978).

[51] G. Wunner and H. Herold, Astrophys. Space Sci. **63**, 503 (1979).
[52] V. Pavlov-Verevkin and B. Zhilinskii, Phys. Lett. A **78**, 244 (1980).
[53] J. Avron, I. Herbst, and B. Simon, Commun. Math. Phys. **79**, 529 (1981).
[54] J. E. Avron, I. W. Herbst, and B. Simon, Phys. Rev. A **20**, 2287 (1979).
[55] H. Herold, H. Ruder, and G. Wunner, J. Phys. B **14**, 751 (1981).
[56] B. R. Johnson, J. O. Hirschfelder, and K.-H. Yang, Rev. Mod. Phys. **55**, 109 (1983).
[57] P. Droz-Vincent, Phys. Rev. A **52**, 1837 (1995).
[58] H. Georgi, Phys. Lett. B **240**, 447 (1990).
[59] E. Eichten, K. Gottfried, T. Kinoshita, K. D. Lane, and T.-M. Yan, Phys. Rev. D **21**, 203 (1980).
[60] W. Lucha, F. F. Schoberl, and D. Gromes, Phys. Rep. **200**, 127 (1991).
[61] N. Brambilla, A. Pineda, J. Soto, and A. Vairo, Rev. Mod. Phys. **77**, 1423 (2005).
[62] K. Marasinghe and K. Tuchin, Phys. Rev. C **84**, 044908 (2011).
[63] K. Tuchin, Phys. Lett. B **705**, 482 (2011).
[64] D.-L. Yang and B. Muller, J. Phys. G **39**, 015007 (2012).
[65] Y. Simonov, B. Kerbikov, and M. Andreichikov, arXiv:1210.0227.
[66] Y. A. Simonov, Phys. Rev. D **88**, 053004 (2013).
[67] M. A. Andreichikov, B. O. Kerbikov, V. D. Orlovsky, and Y. A. Simonov, Phys. Rev. D **87**, 094029 (2013).
[68] C. Machado, F. Navarra, E. de Oliveira, J. Noronha, and M. Strickland, Phys. Rev. D **88**, 034009 (2013).
[69] J. Pirenne, Arch. Sci. Phys. Nat. **28**, 233 (1946).
[70] J. Pirenne, Arch. Sci. Phys. Nat. **29**, 121 (1947).
[71] J. Pirenne, Arch. Sci. Phys. Nat. **29**, 207 (1947).
[72] J. Pirenne, Arch. Sci. Phys. Nat. **29**, 265 (1947).
[73] V. Berestetskii and L. Landau, Zh. Eksp. Teor. Fiz. **19**, 673 (1949).
[74] V. Berestetskii and L. Landau, Zh. Eksp. Teor. Fiz. **19**, 1130 (1949).
[75] R. A. Ferrell, Phys. Rev. **84**, 858 (1951).
[76] M. Deutsch and E. Dulit, Phys. Rev. **84**, 601 (1951).
[77] M. Deutsch and S. C. Brown, Phys. Rev. **85**, 1047 (1952).
[78] R. Karplus and A. Klein, Phys. Rev. **87**, 848 (1952).
[79] O. Halpern, Phys. Rev. **94**, 904 (1954).
[80] V. Hughes, S. Marder, and C. Wu, Phys. Rev. **106**, 934 (1957).
[81] M. L. Lewis and V. W. Hughes, Phys. Rev. A **8**, 625 (1973).
[82] S. Berko and H. N. Pendleton, Annu. Rev. Nucl. Part. Sci. **30**, 543 (1980).
[83] S. G. Karshenboim, Int. J. Mod. Phys. A **19**, 3879 (2004).
[84] T. Kawanai and S. Sasaki, Phys. Rev. D **85**, 091503 (2012).
[85] J. Beringer *et al.* (Particle Data Group), Phys. Rev. D **86**, 010001 (2012).
[86] S. Chatrchyan *et al.*, J. High Energy Phys. 05 (2012) 063.
[87] F. Gurin, Eur. Phys. J. C **49**, 143 (2007).
[88] M. Strickland, Phys. Rev. Lett. **107**, 132301 (2011).
[89] M. Strickland and D. Bazow, Nucl. Phys. **A879**, 25 (2012).
[90] K. L. Haglin, arXiv:nucl-th/0205049.
[91] T. Barnes, S. Godfrey, and E. Swanson, Phys. Rev. D **72**, 054026 (2005).
[92] S. F. Radford and W. W. Repko, Phys. Rev. D **75**, 074031 (2007).
[93] W. W. Repko, M. D. Santia, and S. F. Radford, arXiv:1211.6373.
[94] A. Laschka, N. Kaiser, and W. Weise, Phys. Lett. B **715**, 190 (2012).
[95] I. Sudiarta and D. Geldart, J. Phys. A **40**, 1885 (2007).
[96] M. Strickland and D. Yager-Elorriaga, J. Comput. Phys. **229**, 6015 (2010).
[97] M. Margotta, K. McCarty, C. McGahan, M. Strickland, and D. Yager-Elorriaga, Phys. Rev. D **83**, 105019 (2011).